UNIVERSITY OF NAIROBI

ANALYSIS OF HEAVY METALS, MINERALS AND RADIONUCLIDES IN HEAVY SANDS FROM TIVA AND MWITA SYANO RIVERS, KITUI COUNTY

BY

KOECH NEHEMIAH KIPKIRUI

S56/74430/2012

A Thesis Submitted in Partial Fulfillment of the Requirements for Award of the Degree of Master of Science of the University of Nairobi.

2017

DECLARATION

I declare that this thesis is my original work and has not been submitted elsewhere for examination, the award of a degree or publication. Where other people's studies has been used, this has been properly acknowledged and referenced in accordance with the University of Nairobi's requirements.

Signature…… Date……

Koech K. Nehemiah

S56/74430/2012

This thesis has been submitted with the approval of my supervisors:

	Signature	Date
Mr. David M. Maina Institute of Nuclear Science & Technology University of Nairobi P. O Box 30197-00100	……	……
Prof. Michael J. Gatari Institute of Nuclear Science & Technology University of Nairobi P.O Box 30197-00100	…….....	…… …..

DEDICATION

This work is dedicated to my beloved wife Debra and my daughters; Sherwin and Sheryl, my parents, brothers, sisters and friends for their moral and financial support, understanding, sacrifice and patience during the period of this study.

ACKNOWLEDGEMENTS

My sincere gratitude goes to God whose mercies have enabled me to carry out this research successfully. Also, for His boundless care extended to all those who facilitated this research to its completion.

I would like to thank my supervisors; Mr. David M. Maina for his dedicated time in guiding me through the entire process of research and whose positive critic brought out the best in my work and Prof. Michael J. Gatari with whose assistance enabled me to use the XRD machine in mineral sands analysis and for his support and guidance in the entire process of this research. I am humbled in recognizing the efforts of Prof. Eliud Mathu whose idea provoked the entire research process and for his guidance in the sampling process. I will not forget to mention Prof. Michael Muia and Mr. Michael Mangala for having guided me through my coursework.

I would wish to extend my gratitude to Mr. Simon Bartilol who guided me in laboratory work and my entire class of 2011/12 MSc. nuclear science for their support. My gratitude also goes to the staff at the Institute of Nuclear Science and Technology, University of Nairobi, for making my stay enjoyable and World Agroforestry Centre's staff for their input in mineral sands analysis.

I am also thankful to Kenya Nuclear Electricity Board (KNEB) under the Ministry of Energy and Petroleum for their sponsorship in my 1st-year studies and National Council for Science, Technology and Innovation (NACOSTI) for funding this research.

ABSTRACT

Rivers have been and always will be the source of livelihood to many people, wildlife and aquatic organisms across the world. They are the sources of water for household use, irrigation and watering of both domestic and wild animals. They also provide a home to both aquatic animals and plants. In addition, human activities such as farming and sand mining for both minerals and for building and construction industries among others are carried out in the rivers during the dry spell. Owing to these and many more importance, proper management and exploitation of rivers are of great concern for the welfare of all its dependants.

This research focused on characterizing sands from Tiva and Mwita Syano Rivers in Kitui County. The objective of this research was to analysis river sands for the presence of mineral sands, radionuclides and heavy metals. Ten sand samples collected from river Mwita Syano were analyzed for mineralogical content using the XRD technique while thirty-nine sand samples from the same were analyzed for the presence of heavy metals using EDXRF respectively. Finally, thirty-five sand samples from river Tiva were analyzed for the presence of radionuclides by high-resolution gamma radiation spectrometry using HP Ge detector.

The XRD analysis of river Mwita Syano sand samples indicated the presence of minerals: albite, diopside, hornblende, microcline, quartz, magnetite, orthoclase and ilmenite. The average amount of quartz was the highest with 52.7 % while orthoclase had the lowest with an average of 1.1 % indicating the potentiality of heavy sands as a source of some of the minerals. However, the viability of the heavy sands as the source of minerals requires additional knowledge on the size of the deposit, the cost of mineral separation, infrastructure network and marketing strategies. Hence, this research only opens up the gates for further detailed prospective research work.

The level of primordial radioactivity of river Tiva sands showed the mean specific activities of ^{238}U, ^{232}Th and that of ^{40}K in heavy sands as 8.8 Bq kg^{-1}, 199 Bq kg^{-1} and 329 Bq kg^{-1} respectively. The observed high level of thorium is as results of the presence of monazites or heavy minerals bearing thorium atoms in their structures. The associated absorbed dose rate was 150 nGy h^{-1} which translates to 0.18 mSv yr^{-1} annual effective dose. The radiological hazard indices were found to be within the accepted international commission on radiological protection limits except for representative index level.

The most abundant element in heavy sands was iron followed by titanium. Manganese, vanadium, lead, copper, zinc, chromium, zircon, cobalt and strontium were found to be present in parts per million. In addition, nickel and arsenic mean concentrations were below the minimum detection limits. The average concentrations of heavy metals except those of Pb and Zn exceeded the sediments' recommended values of Wisconsin Guidelines on Consensus-Based Sediment Quality. The mean concentrations of Fe, Zn and Pb were found to be less than the values of 'average shale' while the rest exhibited higher values. Most of the enrichment factors (EFs) calculated ranged from 0.24 to 3.77, indicating deficiency to moderate enrichment of heavy sands by heavy metals. The river sands were found to be very highly enriched with Co (EF of 17.36). The geo-accumulation index (I_{geo}) calculated showed I_{geo} of -3.0 for Pb on the lower side and 3.15 for Co on the upper side corresponding to unpolluted to strongly polluted with the respective heavy metals.

TABLE OF CONTENTS

LIST OF TABLES

LIST OF FIGURES

LIST OF ABBREVIATIONS AND ACRONYMS

AXIL- Analysis of X-ray spectra by Iteration Least-square fitting

CBSQG-Consensus-Based Sediment Quality Guidelines

CEMBS- Central Eastern Segment of the Mozambique Belt

EDXRF-Energy Dispersive X-Ray Fluoresce

EF- Enrichment Factor

FP- Fundamental Parameter

FWHM-Full Width at Half Maximum

GPS- Global Positioning System

HPGe- Hyper Germanium detector

IAEA- International Atomic Energy Agency

I_{geo}- Geo-accumulation Index

INST- Institute of Nuclear Science and Technology, University of Nairobi

Ktpa - kiloton per annum

MCA-Multi-Channel Analyzer

PDF- Powder Diffraction File

RIVM-Dutch acronym for National Institute for Public Health and the Environment

Si (Li)-Silicon detector doped with Lithium ions

$T_{1/2}$-Half life

XRD- X-Ray Diffraction

CHAPTER ONE

INTRODUCTION

1.1. Background

Rivers are central to many beneficial activities that concern the society. They carry water and nutrients around the world and leave valuable deposits of sediments such as sands and gravels. River valleys and plains where deposits form provide fertile soil for farming where irrigation could be practiced. Furthermore, rivers provide nourishment and habitat for many aquatic rare plants and trees e.g. reeds and various kinds of fish amongst other organisms (Fagbote & Olanipekun, 2010). Rivers provide water for various purposes not limited to human and wildlife consumption, irrigation in agriculture and cooling systems in industries. The proximity requirement to river resources has enabled and facilitated the establishment of many cities along the river banks. Nowadays, most of the large cities are located on the banks of the rivers. Bigger rivers are also used for recreation; tourists attraction, fishing, and generation of electricity. Therefore, rivers require a sound minded care for the benefits of the society.

The immense importance of rivers to the society has compelled hydrologists, engineers, and ecologists among others to research on how to safeguard it from pollution for the benefits of the current and future generations. This is because the river ecosystems had suffered from the consequences of both natural and anthropogenic activities, as these environment has acted as an ultimate sink for surface runoff, leaching and effluent discharges (Carlos *et al*., 2014). Natural causes include weathering of rocks and degradation of vegetative cover by natural calamities. For instances, fire due to volcanic eruption causes a massive destruction of natural vegetation cover. Natural release of dangerous gasses e.g sulfur to the atmosphere can lead to the formation of acidic rain. The acid-rain water fastens the weathering of rocks resulting in the formation of sediments. These processes combined with erosion results in deposition of sediment and other physical pollutants from the earth's surface in rivers. Anthropogenic activities that have led to river pollution include releasing of industrial discharge into the water bodies and agricultural practices that use fertilizers and pesticides as rainwater drains these chemicals into the rivers (Begum *et al.*, 2009). Furthermore, an increase of population has lead to the increase of domestic wastes in which one way or another

finds their way into rivers (Ministry of Environment and Mineral Resources, 2012). All these processes show how seriously rivers get polluted day by day and therefore, monitoring and proper managing of river resources are of great concern.

The deposited sediments originate from rocks such as the exposed or near surface igneous, sedimentary and volcanic rocks and exist as silt, loose sand and other soil particles (Joshua & Oyebanjo, 2009). Associated with these sediments are mineral sands whose deposits are formed when their enrichment is very high. Many of these mineral sands are opaque and darken the sediment if their concentrations are high and they become of economic importance based on their properties and prevalence. Some of these mineral sands are heavy minerals which may include magnetite, ilmenite, leucoxene, rutile, chromite, garnet, monazite, columbite-tantalum, cassiterite, among others, all of which are raw materials used in the manufacturing of various products. For instance, ilmenite and rutile are used to manufacture snow-white paints, zircon is used in the manufacture of control rods for nuclear reactors while tantalite is used in the manufacture of transistors. Furthermore, cassiterite is used in manufacturing tin cans (Elsner, 2010).

Heavy minerals may contain some radioactive elements in their structure that negatively impact on our environment. Radioactive elements are unstable elements in nature and must undergo radioactivity (the process by which unstable atoms (radionuclides) stabilize themselves through emission of one or any combination of β-particles, α-particles or γ-radiation). Radionuclides are categorized either by the type of radioactive decay or as man-made or naturally occurring or by the radioactive series. Primordial, progeny or cosmogenic constitute the naturally occurring radionuclides (Focazio *et al*., 1998). Gamma radiation from the primordial radionuclides constitutes the terrestrial component of total background radiation. Cosmogenic radionuclides occur as a result of cosmic rays interacting with atmospheric nuclei. Reasonable contents of man-made radionuclides such as cesium and strontium exist as a result of nuclear accidents and nuclear weapon tests (Kannan, 2002). Radionuclides in the environment add up to the total absorbed dose either through ingestion, inhalation or external irradiation.

Radionuclides are ever present in earth's crust and consequently the main sources of the natural background radiation. The long-lived natural radionuclides especially U, Th

and K exist as a complex of oxides, carbonates, vanadates, hydrated oxides, silicates, phosphates and sulphates (Abdi *et al*., 2006). This implies that human beings have, are and will always be in danger of exposure to radiations emanating from within and without the earth (Prasong *et al*., 2007). Usually, the natural activity is of little or no radiological concern. However, anthropogenic activities, e.g. oil and gas exploration and mining augments the natural radiation to levels that compromise life (Osoro *et al*., 2011). The knowledge of radionuclides' level concentration and their distribution in grains sand assist in assessing the radiological risk to the population due to gamma radiation exposure.

Sediments also contain heavy metals whose presence in the environment in high concentrations are treated as pollutants (Duruibe *et al*., 2007). A pollutant is any substance that negatively impacts the environment and may result in loss of life. The pollution menace is prevalently increasing daily in our environment due to an increase of either or both of natural and anthropogenic activities. The pollutants' presence in the environment has to be within accepted limits and to monitor such levels of pollution, we require a good knowledge of the pollution degree through analyzing samples for heavy metals concentration.

The study area of interest were Tiva and Mwita Syano rivers in Kitui County where river sands were investigated for the level concentration of radionuclides, mineral sands and heavy metals. The main reason behind the choice was to access the level of radiation the residents are exposed to as well as evaluating the level of heavy metal concentrations so as to gauge the heavy metal exposure to residents since farming on or along the riverbeds, sand mining for constructions as well as using water drawn from sand holes (sand dams) are some the human activities being practiced by residents on these rivers. Also, the river sands were observed to be dark in color which could be an indication of mineral sands resource or the presence of accessory elements indicating the proximity of mineral rock/deposits within the region (figure 1.1).

Water holes on the riverbed

Vegetables on Side-river during dry season

Dark sands and attracted are magnetites

Figure 1.1. **River sands nature and human activities along river Mwita Syano**.

Kitui County lies within the arid and semi-arid areas in Kenya. Its climate is hot and dry with very erratic and unreliable rainfall. Its long rains period occur in April to May while short rains period are November and December. The rainfall ranges from 500 mm to 1050 mm per year. Most of the natural vegetation has been cleared due to extensive livestock grazing, charcoal burning and bushfires (Kitheka *et al*., 2011). These human activities have exposed the soils and rocks to various forms of weathering and erosions and these rock fragments have been washed into the water streams in the area. This is evidenced by the presence of black sand found in traversing rivers and has prompted the minerals prospection in the area as evidenced by the limestone and coal discovery (Mulwa *et al.*, 2013).

Due to the scarce vegetative cover of the area, large volumes of sands have been transported to the rivers by agents of erosion. These sands are largely well sorted and mature with minimum clay content. These sands have really helped in conserving water for both domestic and agricultural use to the locals during the dry season. For instances, Mwita Syano, Tiva, Mikuyuni rivers have sand dams along their course (Kitheka *et al*., 2011). This also enables the residents to farm along the river banks sand and in the just adjacent arable land. Sand mining in these rivers also takes place but only on the permission granted by Kitui County government.

There is no if not less information known about the radioactivity, the level of heavy metal concentrations and the amount and type of mineral sands from Tiva and Mwita Syano rivers. Therefore, the information from this research will provide a partial solution to that end since more research needs to be done in these fields in order to actualize the facts about the region's radioactivity, heavy metal concentrations and the type and amount of mineral sands. Consequently, ten sand samples from river Mwita Syano were analyzed for mineral sands using x-ray diffractometer with an aim of identifying and quantifying the minerals present where; minerals are identified by their structures. Also analyzed from the same river were thirty-nine sand samples in which the levels of heavy metals were evaluated using the energy dispersive x-ray fluorescence analysis technique. Lastly, thirty-five sand samples from river Tiva were evaluated for radionuclides by high-resolution gamma-radiation spectrometry using HP Ge detector.

1.2. Research Problems

Heavy sands have been known to contain heavy minerals that are economically valuable. The heavy mineral resource is only viable iff it is adequately large in size and contains high percentage mineral contents. To a certain the minerals viability, it is, therefore, necessary to evaluate all the minerals present in the sediments. Indeed it is often the least common accessory minerals that tell most about the sediment's provenance. The information from the study will partially be useful in mapping out the mineral zones in the Kenya.

Apart from heavy sands being a source of heavy minerals, it also provides sand for building and construction of structures. Therefore, the radiological risks posed to the occupants of such structures and general population within the mining areas needs to be assessed in ensuring that the radiation is within the accepted limits. To achieve this, the natural radioactivity of the heavy sands needs to be established.

Sediments are associated with heavy metals which act as pollutants when their concentrations reach high value. Praveena *et al*., (2007) and Atkinmosin *et al*., (2009) shown in their studies that high levels of metal concentrations in the environment have negatively impacted the living organisms' lives. The causes of the upsurge of heavy metals in our environment could be either natural or anthropogenic or both. Anthropogenic sources include both domestic and industrial activities that cause the

increase of heavy metal concentrations either directly or indirectly. These activities may include mining, industrialization among others. Naturally, metals get into the environment via erosion of metal ore bodies. Once the levels of heavy metal rich concentrations, they cause pollution which in turn threatens the life existence of every living organisms that might be associated with it. Therefore, levels of heavy metal concentration in the environment should be of much concern and one way of providing useful information on this subject is through research.

1.3. Research Objectives

1.3.1. Main objective

The main objective of this research was to characterize the river sands collected from Tiva and Mwita Syano in Kitui County with respect to mineral sands, radionuclides and heavy metals.

1.3.2. Specific objectives

- To identify and quantify mineral sands by deploying XRD technique and deduce the economic viability of sands as a mineral resource.
- To evaluate the specific radioactivity of radioactive elements in sand samples using HP Ge detector and to determine the associated gamma-radiation exposure to residents.
- To measure the metal concentrations in the river sands using EDXRF technique in order to determine the level of metal pollution if any.

1.4. Research Justification

Kitui is covered by patchy grass, non-vegetated rock outcrops and few trees. This has exposed the rocks to weathering and erosion agents. Earlier studies done in the area has shown the presence of quartz, garnets and pyroxenes (Kitheka *et al*., 2011; Nyamai *et al.*, 1999). There is a possibility that mineral sands have accumulated in the rivers as evidence by the presence of black heavy sands in the seasonal rivers. Carrying out a research on identifying and quantifying the mineral sands will attest this claim.

Some of these minerals may have radioactive elements in their structures which will expose the residents to radiological risk once such minerals reach high concentration (Parnell, 2003). This will also increase exposure risk to the crew during heavy mineral concentrate transportation. Therefore, it necessary to find if radioactivity from sands poses any danger to human health.

The region's population has increased as evidenced by the recent establishment of various learning institutions e.g. South Eastern Kenya University and Kenyatta University Kitui Campus. Therefore, sooner or later, the strains on the available resources (including rivers) will set in. For instance, the need to feed the increasing population will require improvised farming e.g. one which encompasses irrigation and establishment of fish ponds (Pauw *et al.*, 2008). Such practices require an informed prerequisite knowledge of the existing resource. To achieve this, the level of heavy metals pollution was determined in order to ascertain the health-wise condition for sand dams and fish bond.

1.5. Research Claim

The mineral sands available are economically viable. For that to hold, the mineral's amount present should be around 5% of the mineral grade (Ong'olo, 2001). In addition, the level of heavy metals pollution and natural radioactivity are within the acceptable limits.

1.6. Research Scope

This research was carried along Tiva and Mwita Syano rivers within Kitui County in Kenya. The research details the mineral sands present and heavy metal concentrations in river Mwita Syano sands and the level of radioactivity of river Tiva sands. This research will provide some useful information and conclusions based on the findings.

CHAPTER TWO

LITERATURE REVIEW

Many studies have been done on sediments with respect to mineral sands, natural gamma radiation, and heavy metal concentrations. First, studies on mineral sands have provided information on the minerals genesis, deposition, and their economic importance. Second, the concern on human effects due to radiation has been the main reason for studying high radioactivity levels from naturally occurring radionuclides. Last, the presence of high concentrations of heavy metals in sands is an indicator of their economic importance but these benefits need to be evaluated against their possible unhealthy effects on the environment. Some of the various methods which have been developed over the years and used to extract information on mineral sands, radionuclides and heavy metals include XRD and EDXRF which were basically used in this research. The information from these studies has helped in understanding our environment better and hence enabling a proper care accorded to it that fosters the healthy coexistence of both plants and animals.

2.1. Mineral Sands

Mineral sands exist in all sediments and sedimentary rocks and deposit forms when heavy minerals content reach high concentrations. Sediments are formed from rocks which are broken down into fragments either through the mechanical means of weathering (clastic) or through chemical reactions. Sediments containing minerals are defined as mineral sand placers. The mineral sand placers essentially fall into Alluvial (beaches or rivers) or Aeolian categories based on the mode of deposition (ILUKA, 2008). Alluvial placers are formed when the loose and fine material of silt and clay are cemented. Examples of alluvial placers are colluvial, fluvial and glacial placers. They are formed along the rivers and beaches through the settling down of heavy minerals when the energy in the transport medium decreases. Fluvial placers form when rocks rich in heavy minerals lose their structure and have loose light minerals swept away by erosion (Macdonald, 1983). On the other hand, Aeolian placers are formed when windblown sediments deposit on the ground when the wind-carrying energy decreases. Most of the mineral sand deposits are formed right from the shorelines to many kilometers away as an unconsolidated fossil.

Mineral sands can be classified as either heavy minerals or light minerals depending on their densities. The heavy minerals have a higher density than that of the quartz (2.65 g cm^{-3}) while light minerals have densities less than that of quartz. Rutile belongs to heavy minerals family whose members are garnet, zircon, magnetic, and ilmenite, among others (Eunice *et al*., 2013).

Exploration for heavy minerals involves the positive identification of exploratory surface, sampling and assaying or determining the heavy mineral percentage. The mineral resource assessment involves the quantification of the heavy mineral grade, the mineralogical assemblage and finally the quality of the mineral species (ILUKA, 2008). This determines the viability of the given mineral resource.

The importance of the commercial heavy minerals (zircon and titanium associated minerals) is appreciated in the variety of their applications. The titanium dioxide minerals are rutile (94-98 % TiO_2 and may have impurities such as SiO_2, CrO_5, Al_2O_3 and FeO), ilmenite (35-45 % TiO_2) and leucoxene (TiO_2>70 %) (Elsner, 2010). These TiO_2 minerals are used in the manufacture of welding electrodes, pharmaceuticals, cosmetics and pigments. The pure white pigment obtained from the refinement of TiO_2 is used as an opacifier in paints, paper and plastics. Titanium metal from rutile, synthetic rutile and titanium slag are used in engineering applications, including architectural coatings, defense industries and aerospace among others. In addition, titanium metal is also used in hip replacements and heart pacemakers due to its non-corrosive nature. Owed to its non-corrosive property, titanium metal is also used in corrosive chemical manufacturing and desalination industries. Zircon dioxide (ZrO_2) is principally zirconium mineral and is a raw material used in ceramic industries for the manufacture of opacifiers, zirconium metals, zirconia and zirconium chemicals for various applications (Tyler & Minnitt, 2004; ILUKA, 2008).

Most of the world's largest heavy minerals resources are within Africa (Tyler & Minnitt, 2004). In southern Africa, Mozambique's Chibuto is the world's potential biggest titanium source with an expected output of 14,000 million tons of 4.9 % grade ilmenite. The Moma deposit also in Mozambique has a mid-range ore-grade of 3.1 % of heavy mineral and is estimated to produce 800 Ktpa of ilmenite, 50 Ktpa of zircon and 14 Ktpa of rutile, making it one of the biggest mineral sands producers in Africa. In eastern Africa, Kenya's Kwale-titanium deposit which is located at 50 km southwest

of Mombasa, has a large clay and silt fraction of about 24 %. The Kwale-titanium base projected the total mineral resources to be 143 million tons at an average heavy mineral grade of 4.4 % as at 2015. It is expected to produce 455-kilo tons ilmenite, 85-kilo tons rutile and 32-kilo tons zircon (Titanium base, 2015). Grande Côte in West Africa is an Ilmenite deposit that sits 50 km northeast of the port of Dakar in Senegal and produces 575 Ktpa of ilmenite, 85 Ktpa of zircon, 6 Ktpa of rutile and 10 Ktpa of leucoxene (GMP, 2011).

Studies have shown that quartz forms the bulk of mineral sands and may contain some of the rare elements. In the study done by Anderson (2011) on the potential use of sands found in North Dakota State in the United States of America confirmed the composition of sands to be comprised of 81-98 % silicates with 45-68 % quartz, 1-16 % carbonates, 1-14 % clay mineral and up to 1 % of iron minerals. Another study was done by Marathe (2012) on river Tapti sediments in central India reported the presence of quartz, kaolinites, calcite, vermiculite, palygorskite, micas and gibbsite with quartz as the dominant. In addition, it also reported quartz as responsible for the formation of soil with high silicates content.

2.2. Radioactivity in mineral sands

Radionuclides are almost present in everywhere in our environment and their specific levels of radioactivity are dictated by geological and geographical set-up but normally pose no threat to population unless they have high levels of radioactivity. Sand deposits are formed as a result of the accumulation of weathered and eroded particles of igneous among other types of rocks in which some may constitute the radioactive elements' series of ^{40}K, ^{232}Th and ^{238}U (Mirjana *et al.*, 2009). Some areas in China, India, Brazil and Austria are known to have high background radiation levels (Kannan, 2002). The external radiation levels from monazite sands in India are higher than that of radiation level reported from Brazil due to the high concentration of thorium. The presence of monazite and zirconium metals are associated with high level of radioactivity since they contain either ^{40}K, ^{238}U or ^{232}Th in their structures (Luigi *et al.*, 2000).

Mineral sands formed from igneous rocks are usually associated with higher levels of radiation. Igneous and metamorphic rocks get weathered and eroded upon subjection to factors of soil formation. The rock segregations which may constitute minerals bearing natural radionuclides from the ^{238}U and ^{232}Th series, as well as ^{40}K, are

compacted to form sand deposits (Mirjana *et al.*, 2009). Mineral sands (monazite, zircon, ilmenite) contain significant amounts of radioactive atoms of ^{238}U and ^{232}Th series. Omar and Hassan (2002) reported a higher level of radiation in black sands of Malaysian beaches. The results evidenced that the concentration of natural radionuclides in the black sand was considerably higher than the normal sand beaches.

All mineral sands are known to be naturally-occurring radioactive materials (NORM) due to the existence of ^{232}Th and ^{238}U atoms in mineral structures. Therefore, heavy mineral concentrate (HMC) pose a higher radiological risk to the community around the plant and along the route of transportation and more so those who transport. It is from this perspective that countries, such as Australia have formed a radiation exposure body specifically for the transport of heavy mineral sands. This body regulates and monitors the transportation of heavy minerals to ensure the safety for all stakeholders (ARPANSA, 2008).

Monazite is well spread globally and heavy mineral sands strand-line extend for hundreds of miles. Radioactive monazite sands occur in high content at the peripheries of all the oceans (Ali *et al*., 2001; Malanca *et al*., 1995) and around the lakes and fluvial systems (Gindy, 1961; Hamby and Tynybekov, 2002). Indian beaches alone contain 8 million tons of monazite. Monazite sands are the most radioactive sedimentary deposits and the consequential effective dose rates are up to 270 mSv yr^{-1}, which is about 650 times the world mean value (Eisenbud and Gesell, 1997; Malanca *et al*., 1995).

Ores that contain higher natural radionuclides than those commonly found in the earth's crust got enriched through technological processes (technologically enhanced natural radioactivity (TENR)). Such sources include coal-fired power plants, uranium mining, production of phosphoric acid and fertilizers, mineral sand processing plants, natural gas (Gesell and Prichard, 1975). Luigi *et al*.,(2000) investigated the radioactivity in raw materials and end products in the Italian ceramics industry and reported a figure of > 3000 Bq Kg^{-1} for ^{238}U and >500 Bq Kg^{-1} for ^{232}Th as average concentrations for the mineral sample (zirconium minerals; zircon and baddeleyite). These concentrations exceeded the earth's crust concentration by magnitude order of at most two. Specific activities of sludges and tiles were the lowest. Gamma radiation dose rates near the bulk zircon sands quantities are low and ranged between 1 and 2 µSv h^{-1}. Therefore, minimum precautions are sufficient to minimize the external radiation exposure.

However, appropriate industrial hygiene rules are required to elude internal contamination by zircon powders. Table 2.1 shows the typical world mean specific activities for ^{238}U and ^{232}Th in some commercial ores and minerals (Al-Sulaiti, 2011)

Table 2.1. **Typical world means specific activities of ^{238}U and ^{232}Th in some commercial ores and minerals (Al-Sulaiti, 2011).**

Type of naturally occurring radioactive material	Activity concentration (Bq Kg^{-1})	
	^{232}Th	^{238}U
Phosphate	100	1500
Rutile	200	200
Zircon	600	3000
Pyrochlore	80000	10000
Monazite	30000	40000
Soil	40	40
Ilmenite	1000	2000
Baddeleyite	1000	10000

2.3. Heavy Metals in the Sands

Heavy metals are present in the natural earth's crust. They occur in rocks as ore in various chemical forms such as sulphides or oxides of the metal, from which they are mined as minerals. They are then released into the environment naturally or through anthropogenic activities. Human activities contribute majorly to a high level of concentration of heavy metals as compared to natural causes. In particular, mining activities tend to upsurge the level of heavy metals contamination in the rivers (Duruibe *et al*., 2007). Heavy metals are seeped out and carried by water runoff and downstream to the sea in sloppy areas.

Weathering of rocks containing heavy metals and mining exposes metal-bearing ores to agents of erosion such as water among others. Heavy metals are conveyed in dissolved forms in water or as an integral part of the sediments and may be kept in sediments or leached to underground waters sources, e.g. boreholes, sand dams, nearby wells causing pollution. Sediments provide a habitat for aquatic animals and act as the main nutrient source for aquatic organisms. The level of heavy metal concentrations in

the sediments is increased by both natural and human activities to the level that undermines the healthful nature the environment accord to its inhabitants. Heavy metals accumulate in the upper sediments, exposing the aquatic organisms to dangers that might culminate in their life termination, slows down growth rate and impair kinds diversity (Praveena *et al*., 2007). Therefore, it is imperative to assess the heavy metals concentration as well as their level of enrichment and gauge the level of sediment's pollution by heavy metals (Fagbote & Olanipekun, 2010).

Heavy metals get into our bodies through consumption of contaminated water, food or air. Metals which end-up in plants bioaccumulate in their tissues, endangering the consumers of the plant tissues. Heavy metals, in turn, accumulates in animal tissue, milk as well as in marine living organisms. Humans then get exposed to heavy metals upon consuming contaminated plants' or animals' tissues leading to biochemical disorders (Kabata-Pendis & Mukherjee, 2007). Heavy metal mining workers are occupationally exposed as well as the population living within the mines, industrial sites via air-suspended particulate matters.

Some of the heavy metals are essential in small amounts for biochemical processes in living organisms (Varsha *et al*., 2010). Zinc is vital for male reproduction system and a masculine element balancing copper in the body. Lack of zinc results in anemia and growth retardation (Holum, 1983; Nolan, 2003). Magnesium, on the other hand, is an essential electrolytic constituent of the body fluids, visa vies; interstitial and cell fluids. (Holum, 1983). Iron and copper ions are necessary for the maintenance of normal body function such as synthesis of metalloproteins (Varsha *et al*., 2010).

A few of heavy metals are toxic even at low concentrations while others are harmless even if present in excess amounts and the effects of others are dependable on the level of concentrations. Lead, cadmium and mercury are toxic at low concentrations (Galas-Gorchers, 1991; Vries *et al*., 2007). On the other hand, potassium, gallium, germanium and calcium are harmless to the environment at high concentrations. In addition, iron, titanium, manganese, chromium, vanadium, zinc and copper have a wide range of health complications when present at high concentrations in the environment (Akpon and Thompson, 2013). Iron oxides deposition in Parkinson's disease is associated with large iron intake. Also, these redox active metals ions are known to augment oxidative damage an initiative of cancer and a vital component of chronic inflammatory diseases

(Varsha *et al*., 2010). Furthermore, some naturally occurring radioactive isotopes of non-toxic elements such as Sr, Zr and Rb may cause health complication to the living organisms.

Various human organs are affected differently by a certain heavy metal exposure. Kidneys and bones are the most probable target organs with regard to cadmium exposure. The main dire effects include increased in osteoporosis risk as well as an upsurge in low-molecular weight proteins excretion in urine and lung cancer risk increase in the case of inhalation exposure. Lead is a neurotoxin known for impairment of neurodevelopment in children. Fetuses and breastfed infants get exposed through their mothers during pregnancy and lactation periods. The biological conversion of inorganic mercury to methylmercury a neurotoxin chemical occur in water and soil. Consuming large amounts of contaminated seafood especially fish leads exposure and susceptible niche is the unborn children through their mothers. Therefore, priority is reducing the consumption of contaminated fish from Hg-polluted areas (WHO, 2007).

Ideally, most studies have been done with the assumption that: first, the sands could be the source of minerals since there is upsurge need of minerals worldwide. Second, the level of radioactivity is well below the threshold amount for the radiological risks exposure and lastly, the level metal concentrations present on the environment are well below the pollution levels. Most of the researchers have proved that heavy metals, mineral sands and radionuclides get into the environment through both geogenic and anthropogenic activities. They are washed away by runoff into water ways or leached and deposited in the aquifer bringing into play both beneficial effects in the case of minerals and accessory elements and detrimental effects such as pollution as a result of high deposition of metals as well as high radiation exposure (Duruibe *et al.,* 2007). Therefore, the main objective of this research was to characterize sands from Tiva and Mwita Syano rivers with respect to mineral sands, radionuclides and heavy metals with the hope that mineral sands are mineable, radioactivity levels do not pose any danger to the residents and lastly, heavy metal concentrations are well below the contamination levels.

2.4. Theoretical Framework

2.4.1. Principles of x-ray diffraction

The X-ray diffraction is a vital technique through which structural and compositional information of the unknown is gathered. X-rays through the sample are scattered coherently (Bragg scattering) by point object in a periodic array to produce mutual constructive interference at specific angles. In phase signal is recorded if consecutive peaks of diffracted x-rays waves match. It is from these constructive interferences that we gather information about the unknowns and occurs iff the distance traveled by the parallel x-rays is an integer function of the wavelength. Fitzpatrick *et al*., (2005) described the necessary conditions for Bragg diffraction as follows:

Rays 1 and 1a in Fig. 2.1 strike point object in the first plane while rays 2 and 2a strike the second plane's point objects. They are scattered in different directions but only rays 1', 2', 1a' and 2a' are scattered in phase making them interfere constructively. Constructive interference come about since the incident and diffracted path length difference is zero. Any scattered rays by point objects in the entire plane that are parallel to 1' are in phase with one another resulting in a corresponding increase of diffracted beam, consequently amplifying the concern intensity. For constructive interference of rays scattered by point object in different planes, the path difference must be an integer function of the wavelength of the ray. Therefore, the path difference for the rays 1D1' and 2B2' is expressed as

$$AB + BC = d\sin\theta + d\sin\theta \quad \text{.....2.1}$$

Equation (2.1) defines the path difference for scattered rays 1a' and 2a'. There is no path difference between scattered rays 1' and 1a' or 2' and 2a' (scattered by the atoms in the same plane). Scattered rays 1' and 2' will be in phase iff the path difference is equal to a whole number of wavelengths, i.e.

$$n\lambda = 2d\sin\theta \quad \text{.....2.2}$$

Equation (2.2) is the Bragg's law and forms the core basis of x-ray diffraction mechanism. In diffractometers, the X-ray wavelength λ is fixed leaving the Bragg angle θ and d as the only variable. The space between diffraction planes of atoms determines peak positions while the number of point objects present in diffracting plane determines

the peak intensity. The angles θ at which x-rays are diffracted is a factor of the distance between adjacent planes d.

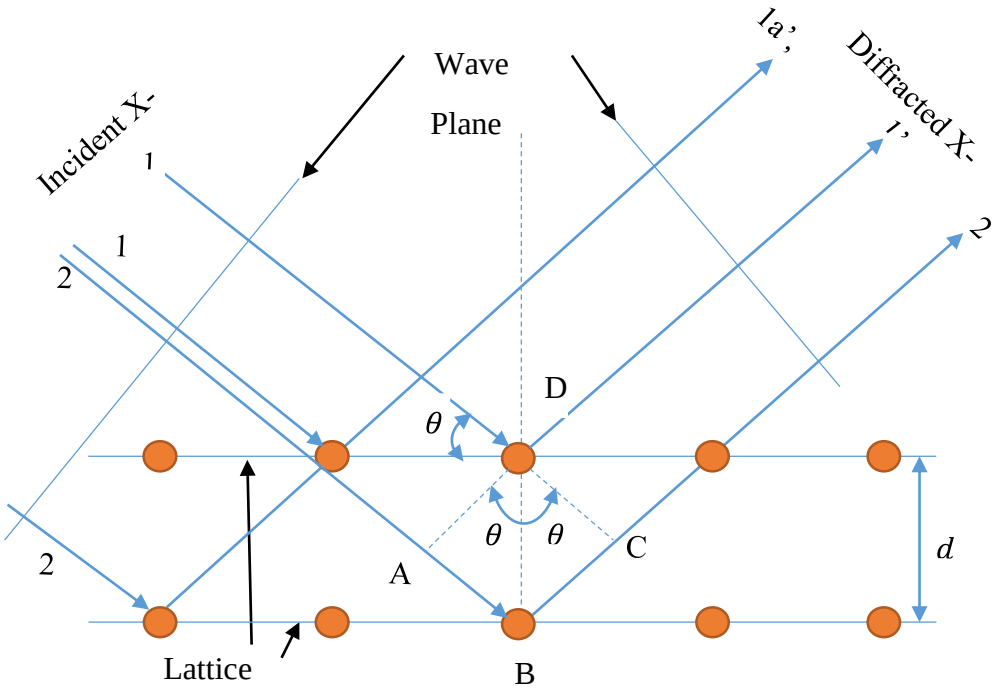

Figure 2.1. **Diffraction mechanism of X-rays by a crystal lattice adopted from Suryanarayana & Norton (1998)**

A powder or polycrystalline sample has millions of crystallites oriented in a random manner. Therefore, there are many crystals oriented correctly for Bragg diffraction for each possible diffraction angle, each giving rise to a cone of diffraction (fig. 2.2). Each cone comprises of many closely spaced dots for each diffraction by single crystalline. Many crystallites oriented randomly produce enough such cone resulting in continuous Debye cone formation. The detector scanning through an arc intersecting each Debye cone in linear diffraction pattern produces a discrete diffraction peak.

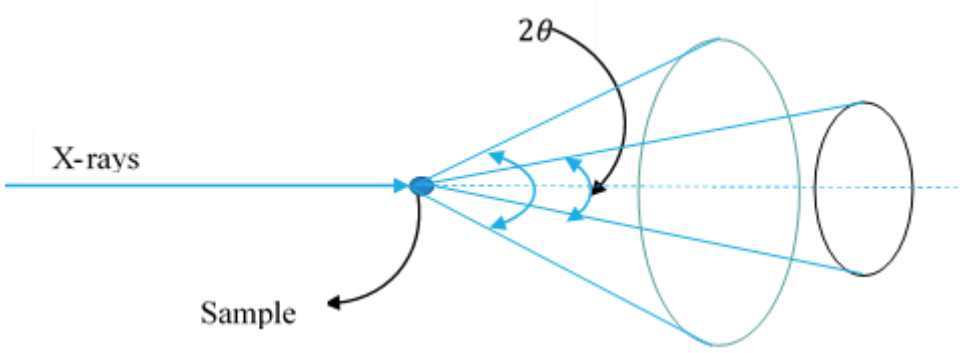

Figure 2.2. **Cone diffraction of a crystal adopted from Mitchel & Perez-Ramirez.**

Powder diffractometers typically use the Bragg-Brentano geometry. The incident angle is always a half of detector angle. In an $\theta:2\theta$insrument, the sample rotates at θ degrees/min and the detector rotates at 2θ degrees/min while the tube fixed. In an $\theta:\theta$ instrument, the tube rotates at a rate -θ degrees/min and the detector rotates at a rate of θ degrees/min while the sample is fixed.

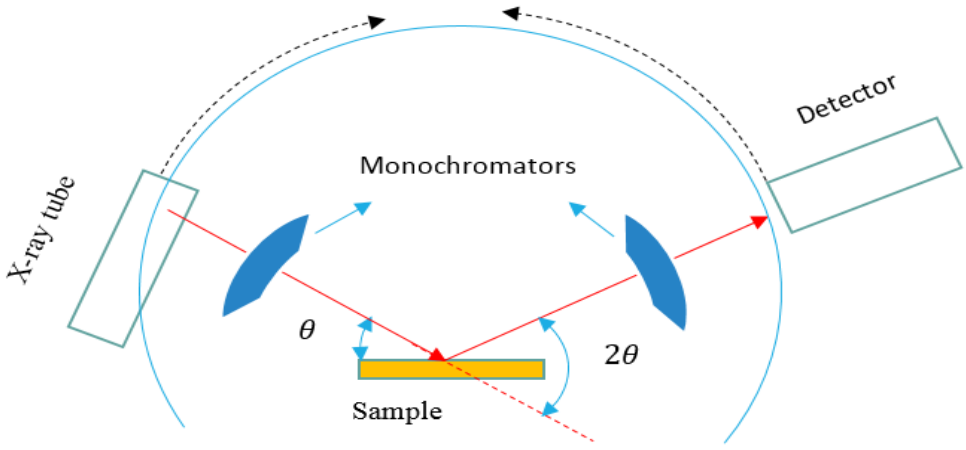

Figure 2.3. **A schematic of Bragg-Brentano geometry adopted from Suryanarayana & Norton (1998)**

Monochromators are used to eliminate unwanted wavelength of radiation from the both incident and the diffracted x-ray beams. Crystal monochromator is used to choose the required radiation wavelength of specific energy. For instance, Kα1 radiation can be selected for the tube source. A diffracted-beam monochromator removes unwanted fluoresced photon, Kβ photons from interfering with the detector reading.

The detector records the angles at which diffraction occurs in lattice planes and intensities of diffracted x-rays beams as it scans the sample along a circle collecting all possible data. The angular positions (2θ) and intensities of the diffracted peaks are plotted to yield a two dimensional pattern. Each peak represents the x-ray beam diffracted by a set of lattice planes (*hkl)* and pattern represent the analyzed material's characteristic. It is from this fingerprints that the unknown is identified by referencing the unknown to the already existing library of powder diffractograms.

2.4.2. Working principles of EDXRF

X-rays lies in between ultraviolet and gamma radiation in the electromagnetic spectrum and their wavelength ranged in between 0.1 to 100 angstroms which correspond to energy between 100 to 0.1 keV. They are produced by either a radioactive source, an

x-ray tube or synchrotron as either continuous or characteristic line depending on the source. When such X-ray photons fall onto a sample, they either get absorbed (Photoelectron) or scattered by atoms in the sample with (Compton Effect) or without (Rayleigh Effect) loss of energy. X-ray's energy determines the mode of interaction.

If the incident energy of x-ray equals the binding energy of an inner shell or more, an electron is ejected leaving a hole behind. The hole is refilled after a certain lifetime as the excited atom transit to stability. In the photoelectric effect, there is a transfer of electron from the outer shell with energy E_o into the inner shell with energy E_i accompanied by an emission of a characteristic x-ray photon with energy hv given as:

$$hv = E_o - E_i \quad \text{.....2.3}$$

Auger effect may occur but the probability that characteristic x-rays is emitted depends on fluorescence yield determined by the element. In low Z-elements, auger effect dominates. Each element has its own characteristic energy spectrum consisting of the allowed transitions within the atom as a result of x-ray atom excitation.

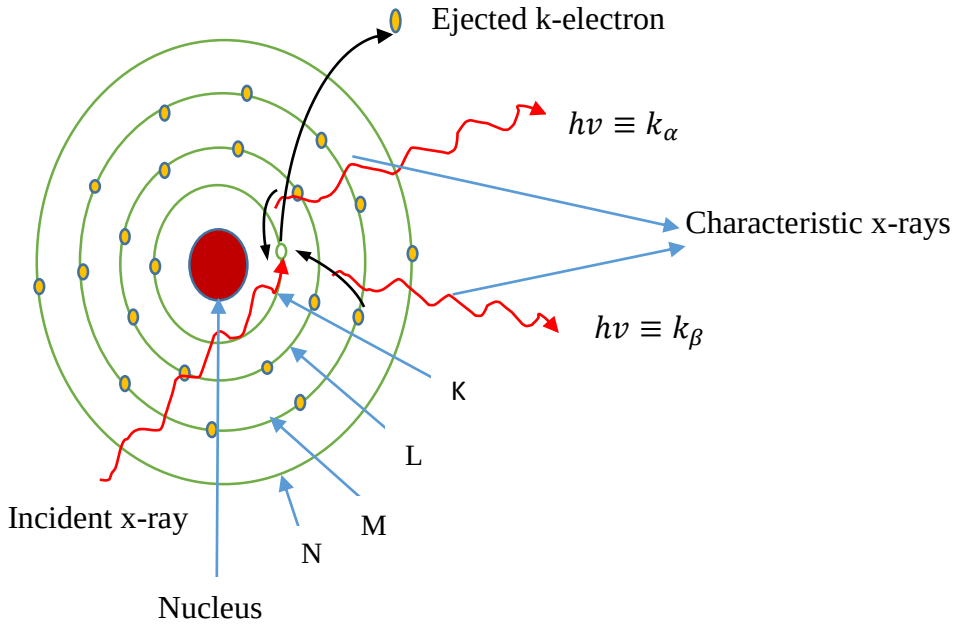

Figure 2.4. **Electron transitions and emitted spectral lines after the K-shell ionization adopted from Jenkin (2000)**

Transitions to the K-shell constitute the k-series; transitions to the L-shell form L-series and so on. The observed characteristic radiations are the unique fingerprints of an element independent of others in the matrix. The energy of each transition from an

atomic shell m to an atomic shell n is proportional to the square of their atomic number as given by the Moseley's law in equation (2.4).

$$E_{mn} = R_H(Z-\sigma)^2\left[\frac{1}{n^2}-\frac{1}{m^2}\right] \quad \text{.....2.4}$$

where R_H is the Rydberg constant, Z is the atomic number and σ is the screening constant of the atom (Meyer, 2000).

Based on Moseley's law, qualitative analysis is possible courtesy of tabulated energy values of characteristic lines. Thus, the elements in the sample are identified from the energy peaks appearing in the spectrum. The peak intensity provides the elemental concentration. A typical spectrum of an irradiated sample has multiple peaks of different intensities each corresponding a specific element. The area under each element's characteristic peaks gives the element's concentration. Fig. 2.5 is an example of such spectrum.

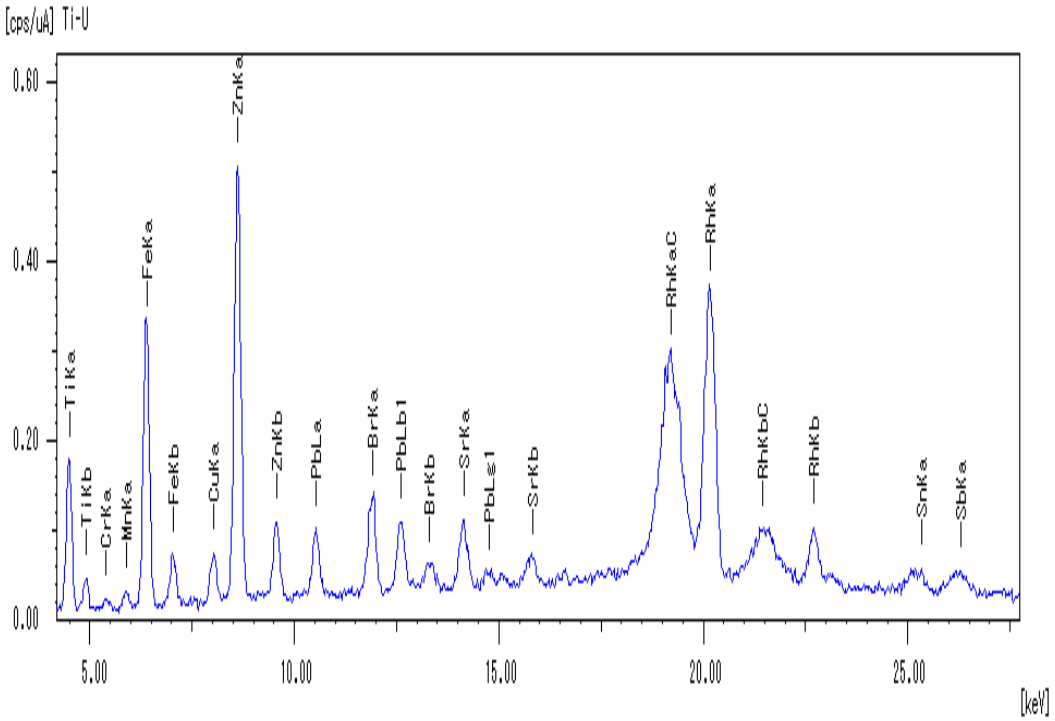

Figure 2.5. **Typical Qualitative and quantitative analysis results obtained by FP method for incinerated ash.**

CHAPTER THREE

MATERIALS AND METHODS

In this chapter, the geology and geography of the study area are described and followed by the various methods of sampling and sample preparation deployed. In addition, the analysis of mineral sands, radionuclides and heavy metals in sands are also discussed. Finally, the respective derivation of specific indicators and their implications of radionuclides and heavy metals are given.

3.1. Study Area

The study areas were Tiva and Mwita Syano rivers around Kwa-Vonza area in Kitui County, Kenya. Kitui County is bounded by the equator and latitude 0° 30' S and by the meridians 38° 00' and 38° 30' E within the fig3.1. Kwa-Vonza Centre is around 165 km from Nairobi along Kitui-Machakos road, around 40 km from Kitui. River Mwita Syano is 3-4 km from Kwa-vonza along Kwa-Vonza-Machakos road while river Tiva is 4-5 km along Kwa-Vonza-Kitui road (Kitheka *et al*., 2011).

3.2. Geology Set-up of Kitui

Kitui falls under the central eastern segment of the Mozambique belt (CEMBS) and forms the eastern part, as described by Nyamai *et al*. (2003). Initially, the region was predominantly considered to consist of migmatites, pelitic and semi-pelitic schists and gneisses. Currently, new lithological units of anorthositic, granitoid, gabbroic to ultramafic intrusions and few andesitic volcanic are widespread in the region. Synformal and antiformal north-southerly oriented with curved axial traces exist as a result of refolding. The Kitui anticline, for example, runs for about 200 km in north-south axial trace and 30 km long limbs on either side of the main axial trace (Mathu & Tole, 1984; Mathu, 1992). CEMBS consist of many neoproterozoic faults, shear zones and thrust, few of which has dimensions regionally. For instance, Yatta shear zone extends for more than 300 km in NW-SE direction.

The geological succession in the Kitui area consists mainly of rocks of presumed Archaean age with a small proportion of post-Archaean rocks (Dodson, 1953). The earlier formations comprise rocks of the Basement System, together with minor intrusions. The younger rocks consist of a sedimentary series of probable Tertiary age,

Miocene kenyte, Nyambeni basalts of Pleistocene age and superficial sediments deposited between Pleistocene and recent times. The basement system in the North Kitui area consists of a vast succession of heterogeneous para-gneisses, quartzites, crystalline limestones, calc-silicate rocks, amphibolites and graphitic gneisses invaded by minor acid and basic intrusive (Dodson, 1953). The geology of the river course is composed of high-grade metamorphic granulites and gneisses rich in garnets and black minerals, iron ore pyroxenes (Kitheka *et al*., 2011).

3.3. Physiography of the Study Area

Kitui physiography is based on the predominant N-S strike and partly on the northwesterly trend of many of the rivers; which are fairly wide and some have steep banks. It has both lowland and highland areas with an altitude of 400 to 1800 m above the sea level. The main feature within the locality of the study area is the Yatta plateau, stretching from north to the south separating the Athi and Tana River basins. The area falls under ecological zones IV (land with less potential for agriculture and has savannah woodland with annual rainfall ranging 500-800 mm) and V (rangeland dominated by Commiphora and acacia species and bushes). The climate of the area is hot and dry with very erratic and unreliable rainfall typical of arid and semi-arid climatic zone. The rain pattern in the region consists of rainy reasons; long rains in April to May and short rains in November to December. The temperature ranges between 16 ^{0}C and 34 ^{0}C with the highest in February. The prevailing wind is generally easterly (Kitheka *et al*., 2011).

Owing to the comparatively low rainfall and to the indigenous practice of overgrazing with both cattle and goats the vegetation is mainly of the thick thorn-bush type with little grass. The lack of a good cover of vegetation, as is especially noticeable in abandoned cultivated patches, due to charcoal burning, tree cutting, fuel wood extraction, has led to serious gully and soil-wash, and some areas in the northwest are severely eroded (Kitheka *et al*., 2011). The erosion surface is an extension of the surface that passes under the base of the lavas of the Yatta plateau. The soil now covering most of the area is a red-brown sandy type and very deep in parts, but of poor fertility.

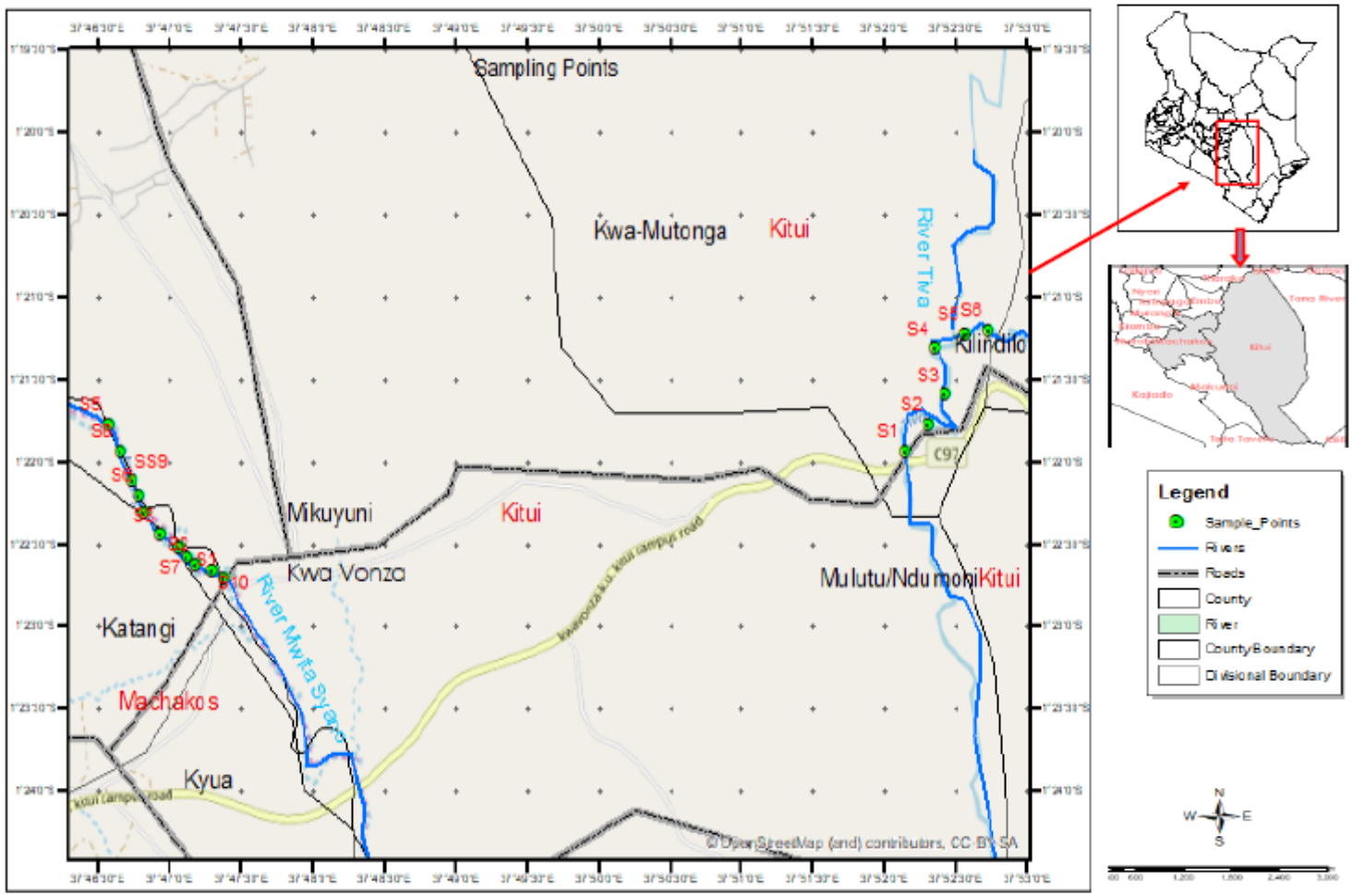

Figure 3.1. **Map showing the sampled area in Kitui**

3.4. Mineral Sands Analysis

Mineralogy analyses involve identification and quantification of mineral species and sometimes revealing the mineral structure. In facilitation of these, various techniques are used depending on the main objective of the research and the merits and demerits of the mode to be chosen. Examples of such techniques are; x-ray diffraction, scanning electron microscopy, an electron or neutron diffraction, Fourier transforms, infrared spectroscopy, chemical analysis, nuclear magnetic resonance, an electron paramagnetic resonance, among others. For this study, however, the mineralogical content of sand was performed using x-ray diffraction technique at the World Agroforestry Centre.

3.4.1. Sampling and sample preparation

A total of ten surface sand samples of up to 10 cm deep were collected from river Mwita Syano for mineral sands analysis. Five of which were collected from the side-deposited sands (side-river samples) and rest were from the middle floor of the river starting at the Kwa-vonza-Machakos road bridge up the stream. The distance between two consecutive sampling sites was around 200 m and mapped by global positioning system (GPS). The side-river sampling sites were selected randomly and mapped using GPS. Ten samples each weighing roughly 1 kg were packaged in well-labeled sample polythene bags were transported to the Institute of Nuclear Science and Technology (INST) for sample preparation and later taken to the World Agroforestry Centre for mineralogical analysis.

The samples were then air-dried at room temperature after which they were sieved through a 2 mm mesh, packed in 100 g sample bag and taken to World Agroforestry Centre. The samples were grounded and thoroughly mixed for homogeneity purposes so as to get a complete sample representative XRD pattern. They were then sieved through a 250-micrometer mesh. Three grams of the sample was micro-milled after topping-up to 12 g with ethanol to preserve the mineral properties using micronizing milling machine for 12 minutes. Thereafter, the mixture was centrifuged for 10 minutes at 4000 revolutions per minute to separate heavier part from lighter (ethanol) and decanted. Finally, to the heavier part, 3 drops of hexane was added to deter normal-oriented preference, thoroughly mixed using the vortex mixer and left overnight to dry. The dry prepared sample was loaded on the disc holder, tamped severally using a razor blade to blend the preferred orientation and leveled ready for analysis.

3.4.2. Sample analysis

Samples were analyzed using x-ray diffraction technique. The XRD equipment requires the expertise and must be used with caution to minimize cumulative x-ray radiation exposure. Fortunately, modern equipment has been designed to eliminate such dangers (Deng *et al*., 2009).

Powder x-ray diffraction technique suits the crystalline mixture analysis perfectly since each constituent of the mixture yields its own characteristic pattern enabling multiple identifications of the components by disentangling their patterns (Chadima *et al*., 2003). X-ray through the sample fixed on the goniometer axis gets refracted by sample's crystal lattice planes. The variations in the diffracted x-ray intensities are detected, measured, recorded and plotted against the rotation angles (Bragg angles) to yield x-ray diffraction pattern (diffractogram) of the sample as depicted in Fig. 3.2 below (Corbell, 2004).

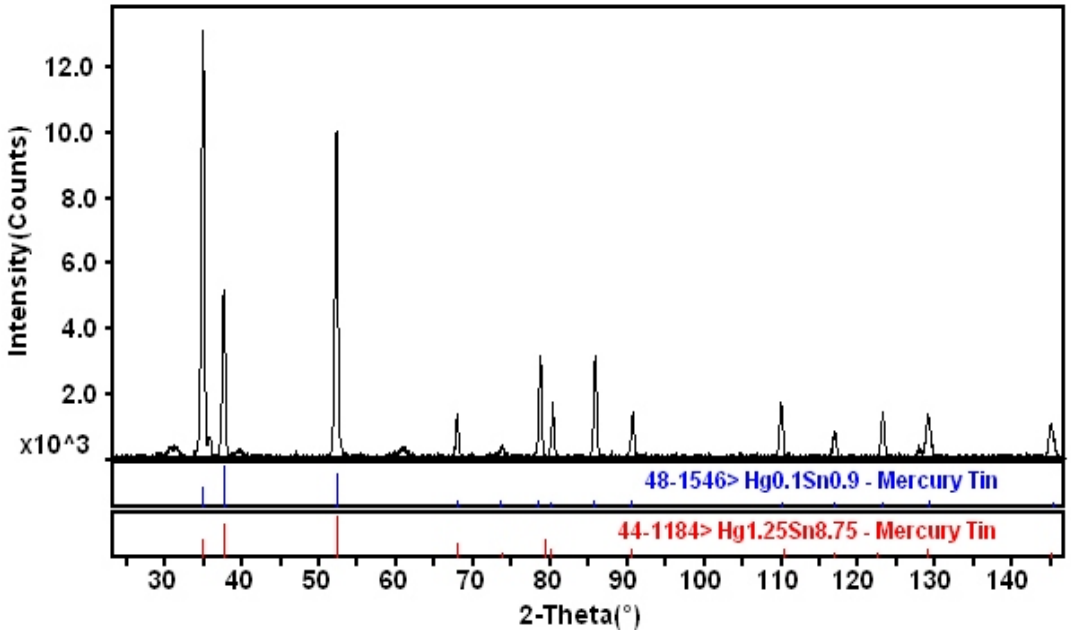

Figure 3.2. **Metal fillet and stick x-ray patterns for the mercury-tin compounds (PDF database)**

Positions and intensities of the recorded pattern are then analyzed with regards to quantitative (frequency of phases), qualitative (phases not elements) and the lattice constant using appropriate computer software. The resulting XRD data are referenced to powder diffraction patterns (over 200,000 of crystalline phases) found in the powder diffraction file (PDF) database. It is from referencing that the mineral is identified. The

PDF database is supplied by International Center for Diffraction Data (ICDD). The PDF database contains substance name, chemical formula, lattice constants, Miller indices and other crystallographic information. The concentration of a particular phase in a multiphase mixture is proportional to its obtained diffracted intensity (Kamau, 2013).

3.4.3. Instrumentation

The various instrument and materials used right from the sample preparation to the extraction of the XRD data are enlisted in appendix 1. Bruker AXS, D2 Phaser Diffractometer system which operates at 10 mA and 30 kV and equipped with Nickel-filtered Cu-Kα1 radiation was used in mineral sands analysis. The angular measurement ranged from 3 to 75^0 2θ with rotation rate of 15^0/min and accuracy of 0.02 in the entire operation of generating x-ray diffractogram. The instrument enabled the data collection with low sensitivity to sample density variations and high peak to background ratio. The conditions set for the sample analysis were ensured by keeping the 0.334 nm quartz's strongest peaks within the counter linearity range and the beam remained within the lowest 2θ angle. The duration at which the intensity of diffraction of a certain mineral in the investigated sample matrix was recorded lasted for up to 30 minutes as the sample and detector rotates through their respective angles as a peak.

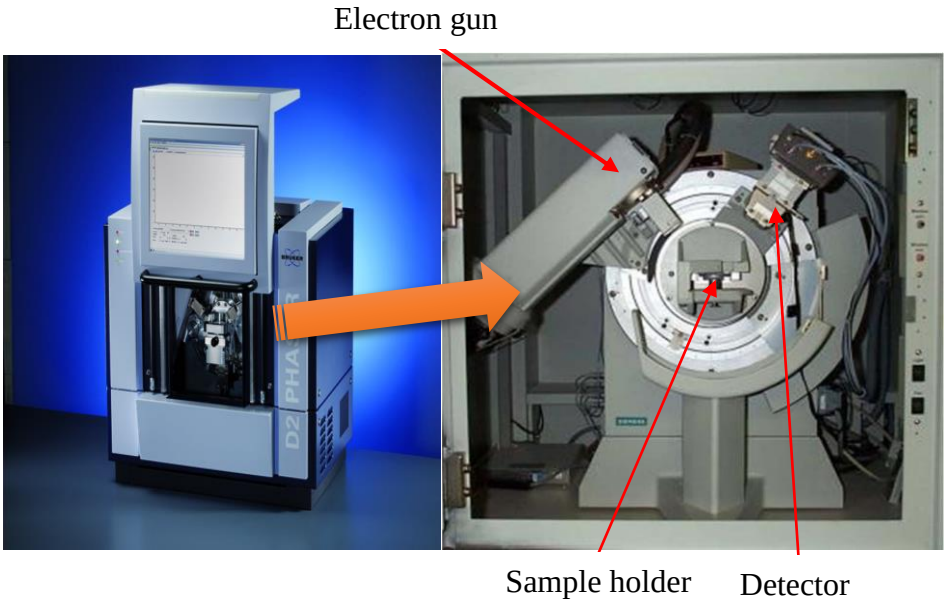

Figure 3.3. **A Desktop Bruker AXS, D2 phaser diffractometer at the World Agroforestry Centre, Kenya**

3.5. Radionuclides Analysis

Measurement of radioactivity in samples determines the level of radioactivity on the actual ground and is generally expressed in Becquerel per kilogram (specific activity). There are various techniques of measuring radioactivity which include gamma spectrometry, alpha spectrometry and low-background gas-proportional beta counting among others. The choice of the technique to be used depends on the type of the radionuclide to be investigated. (Focazio *et al*., 1998). Gamma spectrometry gives the amount of radiation emitted at specified energy levels, enabling the quantitation of the radionuclide under investigation. Solid-state detectors are most used as sensors in gamma spectrometry because of their high sensitivity. Gamma spectrometry was deployed in analyzing for the presence of radionuclides in the heavy sands.

3.5.1. Sampling and sample preparation

Sand samples were collected randomly along the river Tiva and their coordinates recorded using a handheld GPS. A shovel and a hand trowel were used in collecting a total of 35 samples comprising of both the surface (0-10 cm deep) and sub-surface (50-70 cm deep) samples. The samples each of about 1 kg were put in sampling polythene bags, labeled accordingly and transported to INST for analysis. They were dried for a month at room temperature. They were then sieved through 2 mm mesh, before being packed in 200 cc plastic containers, completely sealed with aluminum foil and lid to prevent radon from escaping. They were left for five weeks enabling the system to reach secular equilibrium i.e. for the activities of the parent and the daughter to reach equality (^{226}Ra and its daughters and ^{228}Ra and its daughters). Figure 3.4 shows an example of secular equilibrium. Under this condition, the parent radionuclide undergoes a very slow rate of decay with an appreciable change in its activities during many half-lives of its decay products, while daughters grow in and then decay (Al-Sulaiti, 2011). The concentration of the daughter nuclides is then estimated by measuring the gamma ray associated with them using high-resolution gamma spectrometer.

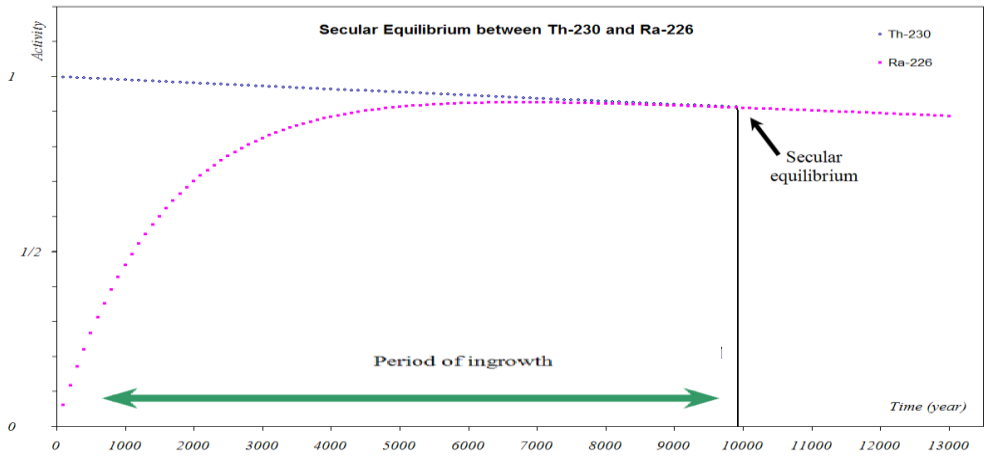

***Figure 3.4*. Secular equilibrium showing how parent ^{230}Th (T1/2=7.738 *10^5 years) and its daughter ^{226}Ra (T1/2=1600 years) decay to reach the point where their activities are equal (Al-Sulaiti, 2011)**

3.5.2. Sample analysis

Gamma ray spectrometry enables the identification and quantification of radioisotope nuclides in the sample mixture. This technique allows detection of several gammas emitting radio nuclei in the sample with little sample preparation. The measurement gives a spectrum of lines (fig. 3.5) of which the amplitude is proportional to the activity of the radionuclide and its corresponding energy is indicated by its position on the horizontal axis (Reguigui, 2006).

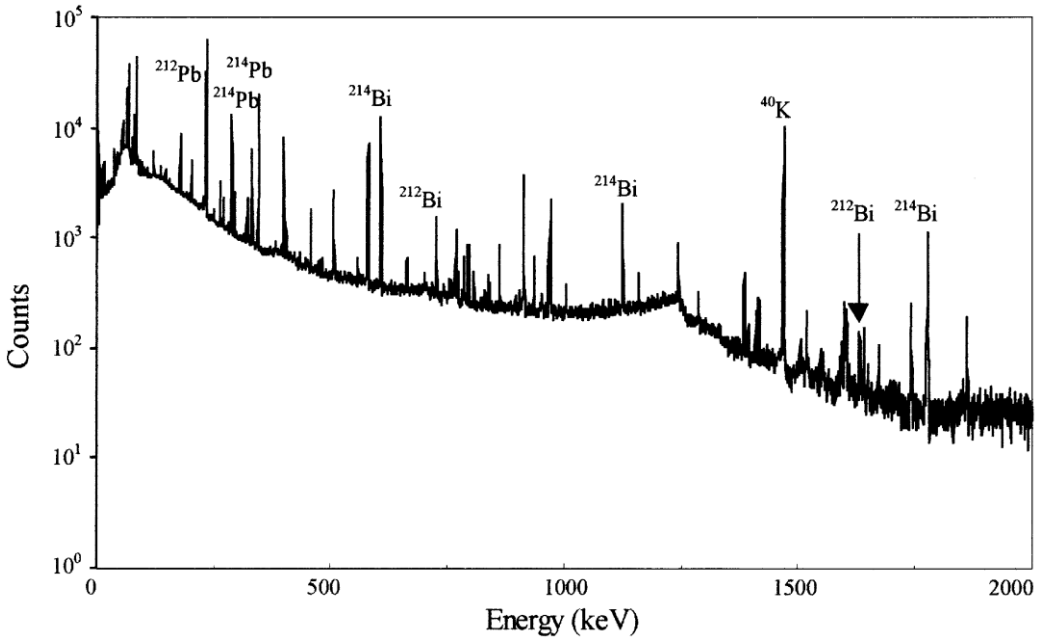

***Figure 3.5*. A typical illustration of gamma-ray spectrum of a ceramic tile (Luigi *et al.*, 2000)**

The gamma ray working system consists of HPGe detector, high voltage power supply, preamplifier, amplifier, analog to digital converter, and a multichannel analyzer. It is applicable in various fields not limited to monitoring in nuclear facilities, health physics, and nuclear medicine, research in materials, bioscience, environmental science and industrial uses of radioisotopes. Due to its wide-range suitability usage, it was employed in this study case to evaluate the radioactivity of heavy sands resource.

3.5.3. Instrumentation

The detector diameter is 57.4 mm, the length is 56.9 mm and with the volume of 144.0 cm^3. The energy resolution (FWHM) of the system is 1.9 keV at 1332.5 keV gamma-ray transition of ^{60}Co with 31.6 % measured efficiency. The spectrometer's energy calibration was performed using a mixture solution of ^{60}Co at 1173.2 KeV and 1332.5 KeV and ^{137}Cs at 661.66 KeV. The detector is housed in a massive lead case to minimize background radiation from interfering with the gamma ray from sample reading. Thermal generation of charges carries is reduced to the acceptable limits by cooling the detector using liquid nitrogen at 77^0K. The liquid nitrogen is kept in a large cryostat (30 L capacity) carefully maintained.

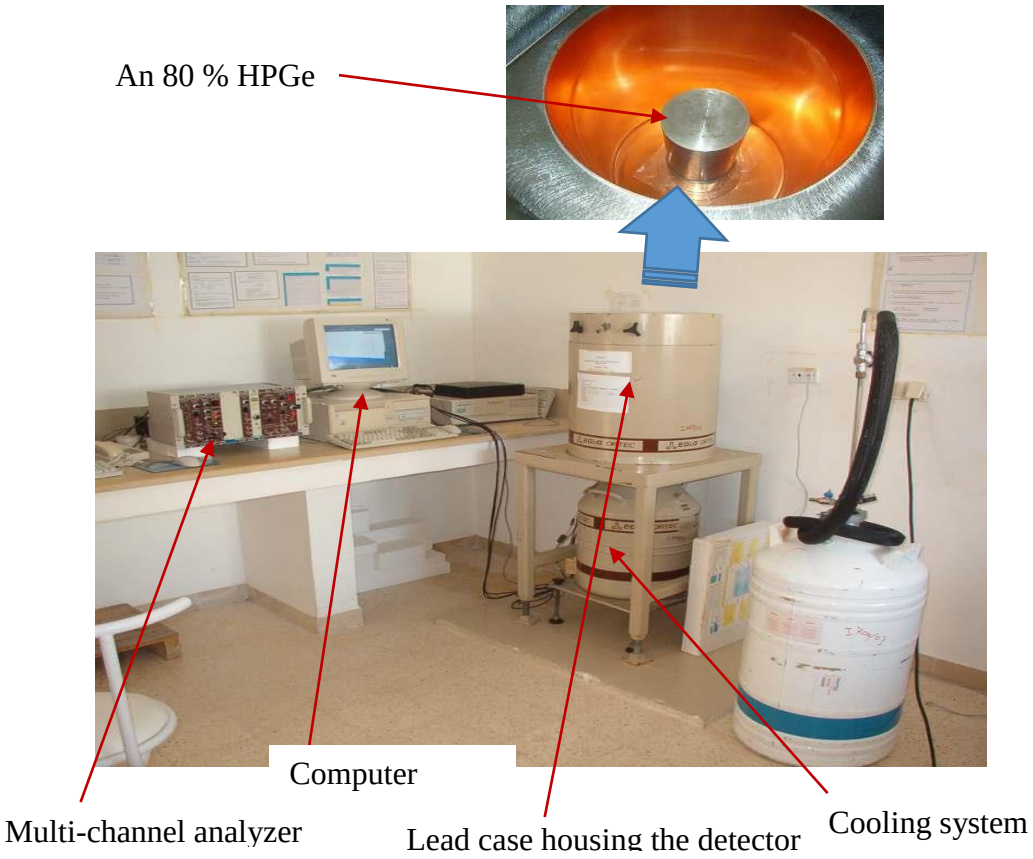

Figure 3.6. **A typical gamma spectrometry work station (Reguigui, 2006)**

The characteristic gamma rays of specific radionuclide under investigation present in the matrix are emitted with one or more well-known energies. The characteristic gamma rays detected are treated by the multi-channel analyzer and shown on the computer in the form of a spectrum (Reguigui, 2006). The system equipped with Maestro Computer Software was used for data acquisition and analysis.

The activity concentration of radionuclides was determined by placing the sand samples on the HPGe detector and counted for at least 10 hours. The activities of the ^{238}U and ^{232}Th were determined indirectly with a using of the gamma lines of the known members found in their respective series. This was accomplished by using gamma lines peaks of ^{214}Pb (351.9 keV) and ^{214}Bi (609.31 keV) for ^{238}U and ^{212}Pb (238.63 keV) and ^{228}Ac (911.07 keV) for ^{232}Th. ^{40}K's gamma line of 1460.8 keV was used in determining its own specific activity (El-Kameesy *et al.*, 2008).

3.5.4. Activity Determination

The activity of the radionuclides was determined by comparing intensities of both the unknown and the known samples. The ratio of the activity of the known sample to that of the unknown is equivalent to the ratio of their intensities (count rates). For this to hold, the unknown and the known source was measured under the same conditions. Therefore, the activity of the unknown is given as:

$$A_u = A_k \frac{I_u}{I_k} \quad \text{.....3.1}$$

where A_u,I_u and A_k, I_k are the activities (Bq) and intensities (cps) for the unknown and the known respectively. Specific activity A_s (Bq kg^{-1}) is given as the activity A (Bq) per unit mass M (Kg). Thus,

$$A_s = {}^{A}/_{M} \quad \text{.....3.2}$$

and replacing for the activity with a specific activity and mass, then equation (3.2) becomes

$$A_{su} = A_{sk} \frac{M_k}{M_u} \frac{I_u}{I_k} \quad \text{..... 3.3}$$

where A_{su} and A_{sk}, M_u and M_k, I_u and I_k are specific activities, masses and intensities in their respective units for the unknown and the known respectively.

The known samples provided by IAEA: RGU-1, RGTh-1 and RGK-1 soils with specific activities of 4940 Bq kg^{-1}, 3250 Bq kg^{-1} and 14000 Bq kg^{-1} respectively, were used to determine the activities of ^{238}U, ^{232}Th and ^{40}K in the samples respectively.

The minimum detection limit (MDL) for each activity was determined using the equation 3.4 (Palmer & McInerney, 1994).

$$MDL = \frac{A}{NC} \times 3.3\sqrt{B} \quad \text{.....3.4}$$

where NC is the net count for a sample of activity A in Bq kg^{-1} and B is the background count below the peak of interest.

3.5.5. Gamma irradiation hazard indices and dose rates estimation

The three gamma irradiation indices calculated were radium equivalent, external hazard index and representative level index. Also estimated was the absorbed dose rate.

(a) Radium equivalent activity (Ra_{eq})

Radium equivalent activity (Ra_{eq}) is used to gauge the risks associated with materials that contain ^{226}Ra, ^{232}Th and ^{40}K in Bq kg^{-1} and is given as the weighted sum of activities of ^{226}Ra, ^{232}Th, and ^{40}K. It's workable on the principality that 370 Bq kg^{-1} of ^{226}Ra or 260 Bq kg^{-1} of ^{232}Th or 4810 Bq kg^{-1} of ^{40}K produce the same gamma dose rate (Kumar *et al.*, 2003; UNSCEAR, 1982, 2000; Beretka and Mathew, 1985), and is calculated using the equation below.

$$Ra_{eq} = 0.077A_K + A_U + 1.43A_{Th} \quad \text{.....3.5}$$

where A_K, A_U, and A_{Th} are the activity concentration of ^{40}K, ^{238}U and ^{232}Th respectively.

(b) External hazard index (H_{ex})

This is the risk estimation of the natural gamma radiation. The focus is to limit the radiation dose to the admissible dose equivalent limit of 1 mSv yr^{-1} and is given by the equation below (Beretka and Mathew, 1985). It should be below the unity.

$$H_{ex} = {}^{A_U}/_{370} + {}^{A_{Th}}/_{259} + {}^{A_K}/_{4810} \leq 1 \quad \text{.....3.6}$$

where all the variables have the same meaning as in equation of radium equivalent.

(c) Representative level index (Iγ)

The representative level index is defined by the equation below

$$I\gamma = {}^{1}/_{150}\,A_U + {}^{1}/_{100}\,A_{Th} + {}^{1}/_{1500}\,A_K \leq 1 \quad \text{.....3.7}$$

where the meaning of the variable does not change. This value must be <1 if the radiation exposure is limited to 1 mSv yr^{-1}.

(d) Absorbed dose rate (D)

The total absorbed dose rate (D) at the height of 1 m above the ground surface was estimated using equation 3.8 (UNSCEAR, 1988).

$$D = 0.662A_{Th} + 0.427A_U + 0.0432A_K \quad \text{.....3.8}$$

where the constants numbers are conversion factors (nGy h^{-1} per Bq kg^{-1}) and variables have the same meaning.

3.6. Heavy Metals Analysis

Most of the methods used in determining element concentrations in sediments are destructive analytical techniques. Example of such techniques are the panoramic techniques; mass spectrometry (ICP-MS) or inductively coupled plasma optical emission spectrometry (ICP-OES) and single element techniques such as atomic absorption spectrometry (AAS). In addition, electrical methods that are also used but destructive include isotope dilution mass spectrometry, fluorometric and spectrophotometric methods. The sample preparation for analysis by either electrical or panoramic techniques are not different (IAEA, 2003). Quality assurance and quality control measures ensure the identity maintenance of the sample throughout the entire process of analysis. Therefore, to preserve the identity, more efficient analytical techniques have been developed to drastically reduce the interference of sample's identity during sample preparation and analysis. Such nondestructive techniques include; neutron activation analysis (NAA), ion beam analysis (IBA), characteristic x-ray fluorescence analysis (XRF). XRF is multi-element analysis technique with sensitivities in the range of 10^{-8} g and it is the technique which was used in the analysis of heavy metals in heavy sands in this research.

3.6.1. Sampling and sample preparation

Sampling was done along river Mwita Syano upstream right from Kwa-Vonza-Machakos Road Bridge. Sampling sites were systematically identified where a total of

39 samples of heavy sands were harvested. Seven samples were collected per site in five sites and the remaining samples were from the side of the river (side-river samples). The sampling points were marked by handheld GPS for mapping purposes. The seven samples per site came about by collecting two samples; surface (0-10 cm top sands) and sub-surface (about 50 cm deep sands) along both side-rivers of the river and three samples; surface (0-10 cm top sands), sub-surface (about 50 cm deep sands) and deep-surface (about 100 cm deep sands) mid-river samples at an interval of 200 m. The side-river sampling was done randomly. All the needed tools such as a shovel, trowel, sampling polythene bags among others were used during the sampling process. The collected samples were taken to INST for sample preparation.

The samples were then air dried at room temperature for a month and sieved through 2 mm mesh to remove coarse particles. The sieved samples were pulverized, sieved again through 75 µm mesh and mixed thoroughly to make the sample homogeneous. Eighty percent of the homogeneous sample was mixed with twenty percent of the binder (starch). Measuring of the sample was accomplished using an analytical balance with precision as low as 0.001 g. Three pellets, each measuring between 0.3 to 0.5 g with a diameter of 2.5 cm, were made from each sample by using collapsible aluminum cups and subjected to 6.5 to 8 tons under an hydraulic press. The prepared pellets were then taken to State Department of Material Science for energy dispersive x-ray fluorescence analysis.

3.6.2. Sample analysis

X-ray fluorescence analysis is a nondestructive method for qualitative and quantitative determination of elemental composition of matrices. It consists of two types depending on their main working principle; wavelength dispersive x-ray fluorescence (WDXRF) and energy dispersive x-ray fluorescence (EDXRF). Both methods are capable of detecting all elements provided that the presence of such element is above its detectable limit in which the x-ray fluorescence can detect. Due to its capability properties, it is used majorly in the elemental and structural analysis. X-ray fluorescence has been used extensively in the various field not only limited to research. In this research, the EDXRF method was employed, where the elements of interest were measured using Titanium-Uranium channel.

3.6.3. Instrumentation

Elemental composition of the pelletized samples was determined using x-ray fluorescence spectrometer; model Shimadzu EDX-800HS CE (212-23701-36) bench top equipment with a Rh anode x-ray tube and a Si (Li) detector. The detector is cooled by liquid nitrogen. The detector is connected to a pre-amplifier, MCA pocket multichannel analyzer and a notebook for data acquisition and evaluation. The Si (Li) detector is mounted at a 45^{o} take-off angle in inverted geometry with respect to the sample and is cooled to -90^{o} C. The current and tube voltage were maintained at 0.35 mA and 50 KV respectively positioned at a 45^{o} incident angle to the sample during irradiation of samples.

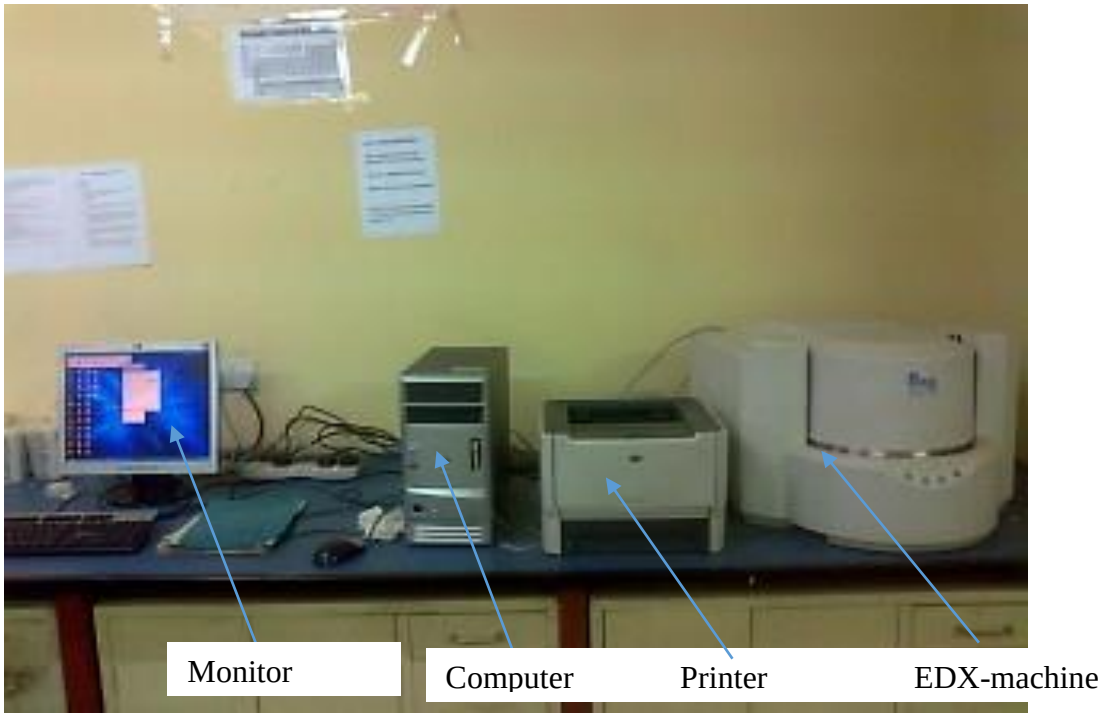

Figure 3.7. **A typical EDXRF work station at the State Department of Material Science, Ministry of Roads and Infrastructure, Kenya.**

The sample was irradiated for a live time of 50 seconds each. For quality assurance, river clay sediments-pt XRF supplied by IAEA was analyzed just the same way samples were treated. Energy calibration was done using standard sample A750, provided together with the EDX-machine. The CuKα energy position and energy resolution were confirmed to be within the recommended value of 8-8.08 KeV and 162.65 eV of FeKα respectively. The detector is combined with a high-count-rate circuit that provides high-precision analysis. The spectra data were analyzed using the AXIL fitting Programme.

To measure the extent to which the sediments are polluted with heavy metals, both the Enrichment Factor (EF) and Geo-accumulation Index (I_{geo}) were determined. EF enables the determination of pollutants' sources as well as helps in assessing the degree of anthropogenic influence (Akpon and Thompson, 2013). EF is defined in the equation (3.9)

$$EF(X) = \frac{(X/N)_{sample}}{(X/N)_{control}} \quad \text{.....3.9}$$

where $EF(X)$ is the EF for the metal X, $(X/N)_{sample}$ is metal X to major metal N ratio concentrations in the sample and $(X/N)_{control}$ is metal X to major metal N ratio concentrations in the reference material such as the control sample. The average shale values from the literature were used as the control (Sutherland, 2000).

The normalization (N) element was taken to be iron because of it small anthropogenic sources as compared to natural sources. Calculating the EF for metal contamination beyond the uncontaminated background levels gives the extent to which the sediment is polluted (Orth and Wells, 2009). The EF values with level of importation of the sediments by metals are as: (Sutherland, 2000)

Table 3.1. **Enrichment Factor (EF) values and their implication**

EF values	**Level of importation**
EF≤1	No enrichment
1<EF≤2	Minimal enrichment
2<EF≤5	Moderate enrichment
5<EF≤20	Significant enrichment
EF>20	Extremely high enrichment

Geo-accumulation index (I_{geo}) quantify the extent to which heavy metal contaminates marine, terrestrial and aquatic environment (Tijani and Onodera, 2009). The I_{geo} of the metal in sediment is determined by:

$$I_{geo} = log_2 \frac{C_{metal}}{1.5B_{metal(control)}} \quad \text{.....3.10}$$

where $C_{metal,}$ is the concentration of the heavy metal in the enriched sample and $B_{metal(control)}$ is the concentration of the metal in the unpolluted sample or control.

The control used was the same as that used for EF for the purposes of comparison. The factor 1.5 minimizes the effect of the possible variation in the background or control values due to lithogenic variation in the sediment (Mediolla *et al.*, 2008). The seven degree of metal pollution evaluation are given in table 3.2 (Huu *et al.*, 2010).

***Table 3.2*. Geo-accumulation indices representing degree of pollution**

I_{geo} values	Degree of pollution
$\boldsymbol{I_{geo}}<0$	Unpolluted
$0\leq\boldsymbol{I_{geo}}<1$	Unpolluted to moderately polluted
$1\leq\boldsymbol{I_{geo}}<2$	Moderately polluted
$2\leq\boldsymbol{I_{geo}}<3$	Moderately to strongly polluted
$3\leq\boldsymbol{I_{geo}}<4$	Strongly polluted
$4\leq\boldsymbol{I_{geo}}<5$	Strongly to very strongly polluted
$\boldsymbol{I_{geo}}\geq5$	Very strongly polluted

Minimum Detection Limit was determined using the equation (3.11) below

$$MDL\ (ppm) = \frac{3\times\sqrt{Ib}}{m\times\sqrt{T}} \qquad \text{3.11}$$

where m is the analyte sensitivity (cps/ppm), Ib is the background intensity (cps), and T is the acquisition live time in seconds (Currie, 1968).

CHAPTER FOUR

RESULTS AND DISCUSSIONS

In this chapter, the results of mineral sands are presented first followed by those of the radionuclides and lastly those of heavy metals. The significance of mineral sands, radionuclides and heavy metals are discussed as well as their distributions in heavy sands. For the radionuclides, the level of primordial radiation was determined and their effective radiation hazard indices calculated. Finally, enrichment factor and geo-accumulation index were used to gauge the level of heavy metals pollution in the heavy sands.

4.1. Mineral Sands

The summary statistics of the minerals present in Mwita Syano river samples are presented in Tables 4.1 and 4.2. The following minerals were observed to be present in the heavy mineral sands: albite, diopside, hornblende, microcline, quartz, magnetite, orthoclase and ilmenite. Quartz was the dominant mineral in both side-river grains of sand and mid-river sands samples. The order of percentage amount of mineral sands in heavy sands were quartz > albite > hornblende > ilmenite > magnetite > microcline > diopside for side-river sand samples and as quartz > albite > hornblende > diopside > orthoclase > ilmenite for the mid-river sand samples. Figure 4.1 shows the corresponding 2-theta value of quartz slightly over 26.7^0 which could be an indication of micas presence in samples (Marathe, 2012).

The high occurrence of quartz is an indication of the presence of igneous rocks in the region. In addition, its significance presence is of economic importance since it can be mined as raw material for the manufacture of both ceramics and porcelains. The quartz percentage amount present ranged from about 32 to 68 and compares well with those obtained in North Dakota region of about 45 to 68 % (Anderson, 2011). The chemical analysis of beach sand zircon and red sediment zircon in India region reported 31 % and 29 % of quartz respectively which is less than the average values obtained in this study. In addition, the values obtained for magnetite and ilmenite in the same region of India were less as compared to the reported in this study (Routray & Rao, 2011).

***Table 4.1*. Summary statistics for minerals in Mwita Syano side-river sands in %**

	Albite	Diopside	Hornblende	Microcline	Quartz	Magnetite	Ilmenite
min	14.1	0	17.8	0	32.6	0	3.2
max	27.3	4.9	21	13.9	58.3	10.9	11.6
1st Qu.	18.8	0	19.1	0	37.3	0	4.8
range	13.2	4.9	3.2	13.9	25.7	10.9	8.4
3rd Qu.	22.6	4.2	19.9	0	49.3	5.3	9.5
median	19.2	0	19.4	0	44.5	3.1	7.3
mean	20.4	1.82	19.44	2.78	44.4	3.86	7.28
SE.mean.	2.2	1.1	0.5	2.8	4.5	2.0	1.5
CI.mean.0.95	6.1	3.1	1.4	7.7	12.5	5.6	4.2
std.dev.	4.9	2.5	1.2	6.2	10	4.5	3.4
coef.var.	0.24	1.37	0.06	2.24	0.23	1.17	0.48

***Table 4.2*. Summary statistics for minerals in Mwita Syano mid-river sands in %**

	Albite	Diopside	Hornblende	Quartz	Orthoclase	Ilmenite
min	17.1	4.1	8.6	51.6	0	0
max	27.9	6.8	13.9	68.7	5.3	2.5
1st Qu.	19.1	4.2	9.3	60.2	0	0
range	10.8	2.7	5.3	17.1	5.3	2.5
3rd Qu.	27.3	6.2	10.2	63.4	0	0
median	22	4.6	9.6	61	0	0
mean	21.96	5.18	10.32	60.98	1.06	0.5
SE.mean	1.87	0.55	0.93	2.8	1.06	0.5
CI.mean.0.95	5.2	1.5	2.6	7.7	2.9	1.4
std.dev	4.19	1.24	2.08	6.21	2.37	1.12
coef.var	0.19	0.29	0.20	0.10	2.24	2.24

The moderate occurrence of albite indicates the presence of granites, alkali diorites as well as alkali feldspar within the region. Its corresponding 2θ angle of 21^0 suggest that it belongs to plagioclase series (fig 4.1). Its significant amount in both side-river and mid-river sand samples is of economic value. It is mainly used in ceramic industries as well as an accessory for other minerals. Its percentage range was comparable to those from the North Dakota region with values of about 10 to 19 %.

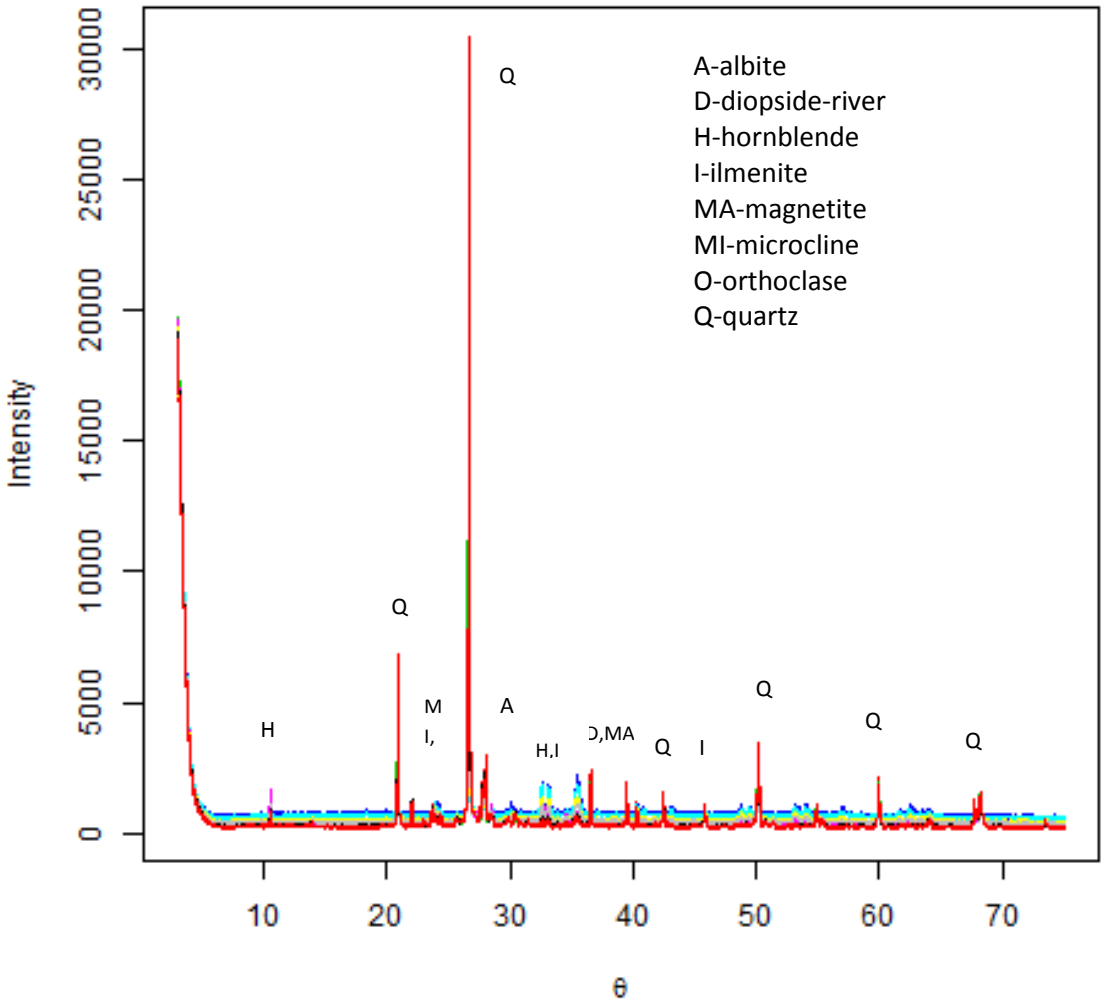

***Figure 4.1*. 2θ Scale diffraction pattern of mineral sands in river Mwita Syano sands**

Orthoclase and microcline indicate the presence of feldspar in the region as well as the presence of high-grade metamorphic rocks, syenites and granite pegmatites. Each one of them was exhibited only in one sample making them hard to depict their distribution in the sands (fig 4.2). Despite their many economic importance, their low occurrence in the sands inhibits the possibility of them being mineable. Both belong to k-feldspar minerals and percentage amounts present were much less the values obtained in North Dakota region of 11 to 20 %.

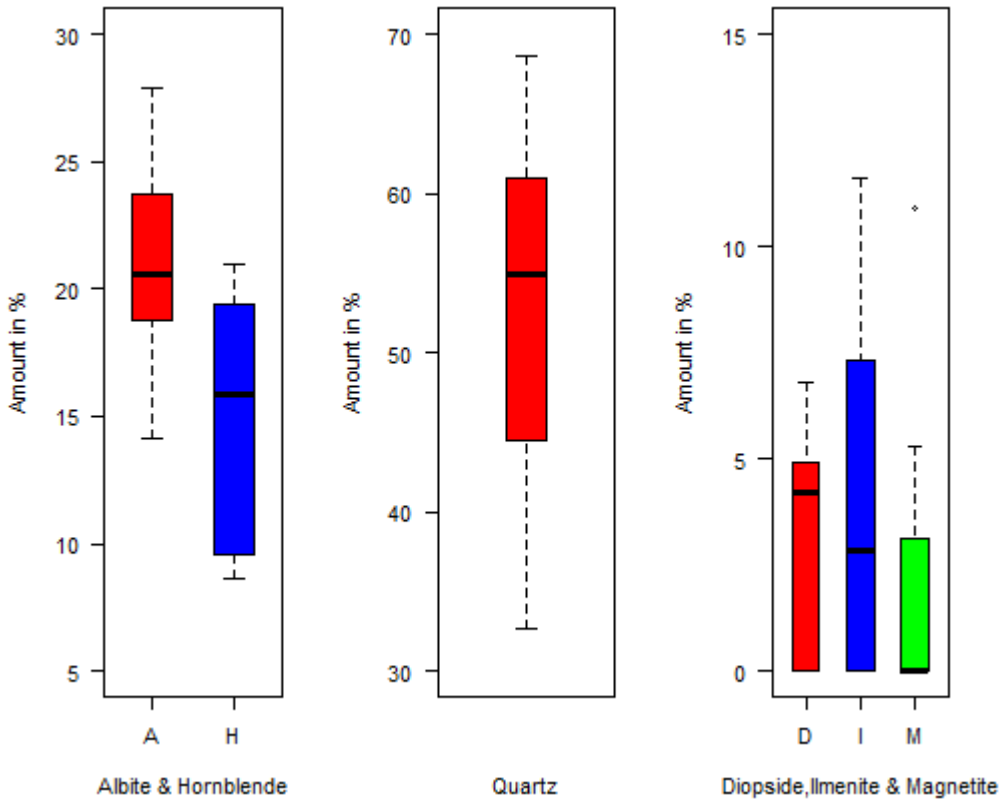

***Figure 4.2*. Combined mineral sands variation in river Mwita Syano sands**

Diopside presence is an indicator of the metamorphic and igneous rocks in the region. It was present in only two of the side-river samples and in all mid-river samples suggesting that diopside is easily carried in water and does not easily deposited. The most significant result of this research was the presence of magnetite in mineable amounts in heavy sands more so in side-river sand samples as compared to those from the mid-river sand samples. It has a strong magnetism property and acts as an accessory mineral in igneous, sedimentary and metamorphic rocks. It's high occurrence in magmatic segregation results in viable placers and hints proximity of large basalt and young volcanoes. There is a possibility that its amount could be increased if heavy sands are concentrated. The size of the mineable sands along the river should be undertaken for it to be confirmed viable. The amount in percentage exceeds those of the North Dakota region of about 1 %.

Ilmenite is an accessory mineral in igneous rocks (gabbro, granites) and metamorphic rocks. It was found mainly in the side-river samples and in only one mid-river sample. The presence in side-river sample reached the mineable amount and can be mined for various uses which include the manufacture of white pigments among others if the

heavy sand volume is sufficiently large. Hornblende indicates the presence of igneous and metamorphic rocks and it was the third commonest mineral in heavy sands after the quartz and albite. The amount found was much higher than those values obtained from North Dakota region of about 2 %. Note that the comparison was done mainly to those from the North Dakota because most the mineral sands found in the river Mwita Syano samples were of the same kind.

4.1.1. Correlation analysis

Correlation information shows if there is any relationship among the analyzed entities. Table 4.3 and 4.4 gives the correlation coefficients of the mineral sands from side-river and mid-river samples respectively. Magnetite and ilmenite relate very strongly in the side-river sand samples suggesting that both minerals may have originated from the same parent rock. Lack of magnetite in the mid-river samples suggest that they are easily carried away by water. Quartz and diopside-river relate well in the side-river samples and poorly in the mid-river samples indicating difference response to factors of leaching but are deposited fairly the same. Albite-ilmenite and albite-hornblende relationships in the mid-river sand samples are positively strong perhaps indicating the same response to leaching factors and differently to deposition mechanism as suggested by poor correlation in side-river samples. There is a strong positive relationship between diopside and quartz in the side-river sand samples and the same can not be said in the mid-river sand samples perhaps suggesting the same response to deposition mechanisms and differently to leaching factors. Diopside relates strongly negative with both ilmenite and magnetite in side-river sand grains suggesting that their origin is different. Both quartz-magnetite and quartz-ilmenite relationships are negatively strong in both side-river samples and mid-river samples indicating different sources. The quartz-hornblende relationship is negatively strong while Ilmenite-hornblende is positively strong in the mid-river samples suggesting the same origin for ilmenite and hornblende but different from quartz.

Table 4.3. **Correlation coefficient for minerals present in Mwita Syano side-river sands**

	Albite	**Diopside**	**Hornblende**	**Microcline**	**Quartz**	**Magnetite**	**Ilmenite**
Albite	1						
Diopside	-0.44	1					
Hornblende	-0.63	-0.14	1				
Microcline	-0.18	-0.41	0.22	1			
Quartz	-0.25	0.88	-0.40	-0.65	1		
Magnetite	-0.002	-0.78	0.68	0.18	-0.76	1	
Ilmenite	0.17	-0.89	0.55	0.36	-0.92	0.96	1

Table 4.4. **Correlation coefficient for minerals present in Mwita Syano mid-river sands**

	Albite	**Diopside**	**Hornblende**	**Quartz**	**Orthoclase**	**Ilmenite**
Albite	1					
Diopside	-0.39	1				
Hornblende	0.71	-0.29	1			
Quartz	-0.84	0.08	-0.82	1		
Orthoclase	-0.38	0.46	-0.27	-0.07	1	
Ilmenite	0.79	-0.49	0.96	-0.84	-0.25	1

4.1.2. **Mineral sands summary outline**

The eight mineral sands found in river Mwita Syano sand samples were: albite, diopside, hornblende, quartz, orthoclase, ilmenite, magnetite and microcline. Quartz was dominant among all. Orthoclase was only found in the mid-river samples while magnetite and microcline were found only in the side-river samples. Table 4.5 gives the summary implications of the results found.

Table 4.5. **Summary outline of mineral sands from river Mwita Syano**

Mineral name	**Amount implications**
Albite	Mineable
Diopside	Mineable
Hornblende	Mineable
Ilmenite	Mineable
Magnetite	Mineable
Microcline	Not mineable
Orthoclase	Not mineable
Quartz	Mineable

4.2. Radionuclides

Background radiation spectrum was used to calculate the minimum detectable activity of ^{238}U, ^{232}Th and ^{40}K as 5 Bq kg^{-1}, 5 Bq kg^{-1} and 30 Bq kg^{-1} respectively. Table 4.6 gives the radioactivity summarized results of river Tiva sands. Uranium radiations from twelve samples were below the minimum detectable limit. It was noticed that the mean surface activities were higher than those of the sub-surface for both the ^{238}U and ^{232}Th (tables 4.6, figure 4.3) which agrees well with the natural radioactivity of beach sands in the Tripoli region. The P-values of 0.5 and 0.7 for ^{238}U and ^{232}Th respectively at 95% confidence interval level were obtained suggesting that the null hypothesis that there is no difference in both surface and subsurface radiation is not rejected meaning the differences are insignificance. Contrary, the ^{40}K surface radiation is less than that of sub-surface with a p-value of 0.1 indicating the insignificance in their difference.

The activity concentration range of ^{238}U is comparable to some beach sands around the world; Northeast Coast, Spain (range of 5-9 Bq kg^{-1}), Valencian Community, Spain (range of 4-16 Bq kg^{-1}), but much less than those from India mainly: less from that of Kalpakkam (36-258 Bq kg^{-1}), Visakhapatnam (100-400 Bq kg^{-1}) (Kannan *et al*., 2001). The activity concentration of ^{232}Th varied the highest. The mean concentration of ^{232}Th is higher than those found in Spain and less than those from India. The activity concentration for ^{40}K varied widely and compared relatively less than those from kalpakkam (358 Bq kg^{-1}) in India. The occurrence of high ^{40}K activity concentration could be indicative of K-feldspar presence in the heavy sands.

Table 4.6. **Summary statistics for the radionuclides in river Tiva sands in Bq kg^{-1} (s=surface, sb=sub-surface)**

	^{238}U_s	^{238}U_sb	^{232}Th_s	^{232}Th_sb	^{40}K_s	^{40}K_sb
min	5.4	6.15	6.12	56.4	155	124
max	14.03	11.72	411	484	649	535
1st Qu.	6.99	6.69	85.6	143	195	236
range	8.63	5.57	404	427	494	411
3rd Qu.	11.19	9.92	314	248	399	501
median	8.28	8.025	177	159.5	233	372
mean	9.15	8.45	205	193	292	365
SE.mean	0.84	0.58	31	25	35	32
CI.mean	1.9	1.3	66	53	75	68
std.dev	2.78	2.03	128	107	146	137
coef.var	0.30	0.24	0.63	0.56	0.50	0.38

Table 4.7. **Comparison of mean activity concentration of river Tiva sands and those of the sands and soils from selected areas in the world ((Prasong *et al.*, (2007); Mirjana *et al.*, (2009); Kannan *et al.*, (2002))**

Country	Region	^{238}U (Bq kg^{-1})	^{232}Th (Bq kg^{-1})	^{40}K (Bq kg^{-1})
Kenya	Tiva (This study)	8.8	199	329
Montenegro	City beach	7.4	9	192
	Great beach 1	15	14	398
	Great beach 2	11	17	412
	Great beach 3	8.9	13.4	338
	Great beach 4	9.6	11.4	276
	Great beach 5	10	12.4	314
	Great beach 6	10.4	12.6	251
Serbia	Lido	7.9	-	299
	Danube river	7.6	-	307
	Belgrade	8.4	-	278
United State	Manhattan, Los Angeles	5.0	17.3	457
	CA city, Santa Monica	11.1	12.5	696
	Great Salt Desert	9.4	11.2	230
Turkey	Patara beach, Xanthos	2.56	10.8	54
Libya	Tripoli-Tayura beach	8.9	4.39	54
	Tariq-city beach	12	8.4	82.4
	Almasif	7	5	62.4
	Janzour	11	3	80.5
India	Kalpakkan	124	1613	358
USA (soils)	Mean	40	35	370
China (soils)	Mean	32	41	440
Spain (soils)	Mean	32	33	470
Worldwide mean (soils)	Mean	32	36	474

The mean concentration of 8.8 Bq kg^{-1} for ^{238}U in sand samples is less than the mean concentration obtained for soils from various part of the world (table 4.7). The mean concentrations of some of the soils around the world ranged from 19-114 Bq kg^{-1} (Abdi *et al*., 2006). The mean concentration for ^{232}Th of 199 Bq kg^{-1} is much higher than the mean concentration of many reported values ranging from 17-95 Bq kg^{-1} while that for ^{40}K of 329 Bq kg^{-1} agrees well with other results obtained from around the world. The mean concentrations for ^{232}Th and ^{40}K were much higher than values obtained in soils from the titanium mining sites in Kenya before mining commences (Osoro *et al.*, 2011). Both ^{238}U and ^{232}Th concentrations are much less than the values of black sands obtained from Pasir Hitam and Batu Ferringhi regions of Malaysian beach of 1150 Bq kg^{-1} and 500 Bq kg^{-1} respectively (Omar and Hassan, 2002). The ^{238}U concentration results agree well with the reported values from Montenegro (City beach and the Great beaches), Serbia (Lido, Danube River), USA (Manhattan Beach, Los Angeles, Great salt desert) and Libya (Mirjana *et al.*, 2009) while that of ^{238}Th concentration was higher than values obtained from the same regions. The ^{40}K concentration agrees only with those from Montenegro but higher than those from other countries mentioned.

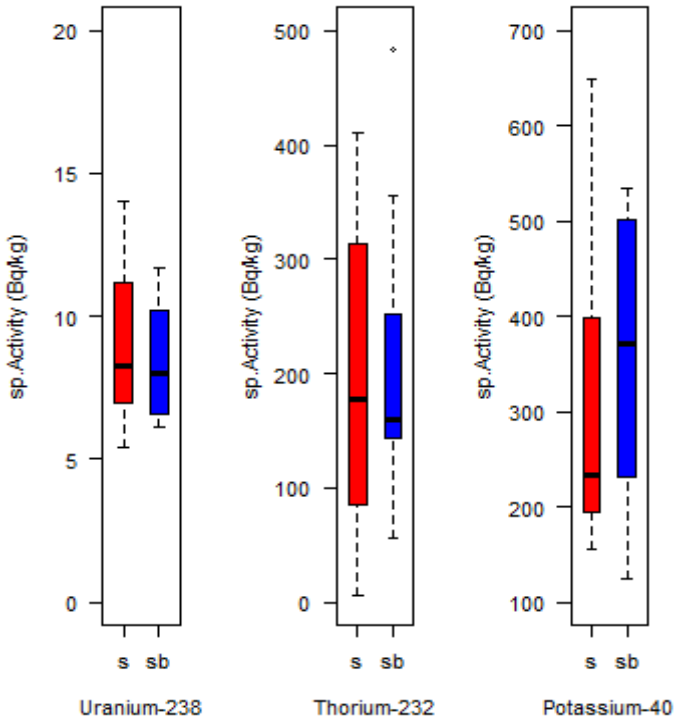

***Figure 4.3*. Surface and subsurface activities for radionuclides in river Tiva sands.**

Among the three natural radionuclides investigated in the heavy sands, the mean concentration of ^{40}K is the highest followed by that of ^{232}Th and ^{238}U recorded the lowest (figure 4.4).

The activity concentrations for ^{238}U and ^{40}K were below the global averages of 50 Bq kg^{-1} and 500 Bq kg^{-1} respectively (UNSCLEAR, 2000). However, the activity concentration for ^{232}Th is almost 4 times that of the global average value of 50 Bq kg^{-1}. The concentration values for ^{40}K and ^{238}U are within the range of the most of the world's activities in various places. The high ^{232}Th value could indicate the presence of minerals bearing radionuclide atoms in their structures (Abdi *et al.*, 2006).

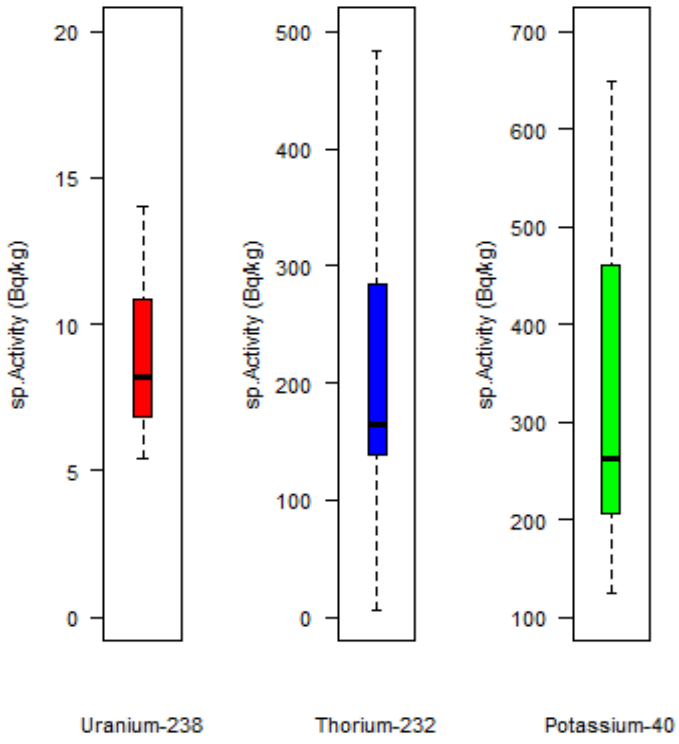

Figure 4.4. **Radionuclides' specific activities in river Tiva sands**

The right side of the river is taken to signify the right-hand side as one walk up the stream while the left side represents the opposite side. The center is the right-left midway. The right side records slightly higher presence of radionuclides as compared to the left side. The mean activity for the right side is 209 Bq kg^{-1} and 190 Bq kg^{-1} for the left side. For the center concentration, 198 Bq kg^{-1} was recorded as the mean. Therefore, the right side of the river could be containing a high level of radioactivity (figures 4.5a, 4.5b).

The distribution of ^{40}K is not widely affected by the course of the river flow since the concentration is evenly distributed along the river. Sites No. 1 and No. 6 have the highest mean specific activities which could suggest the flatness of the river bed at these points as compared to other sampled point.

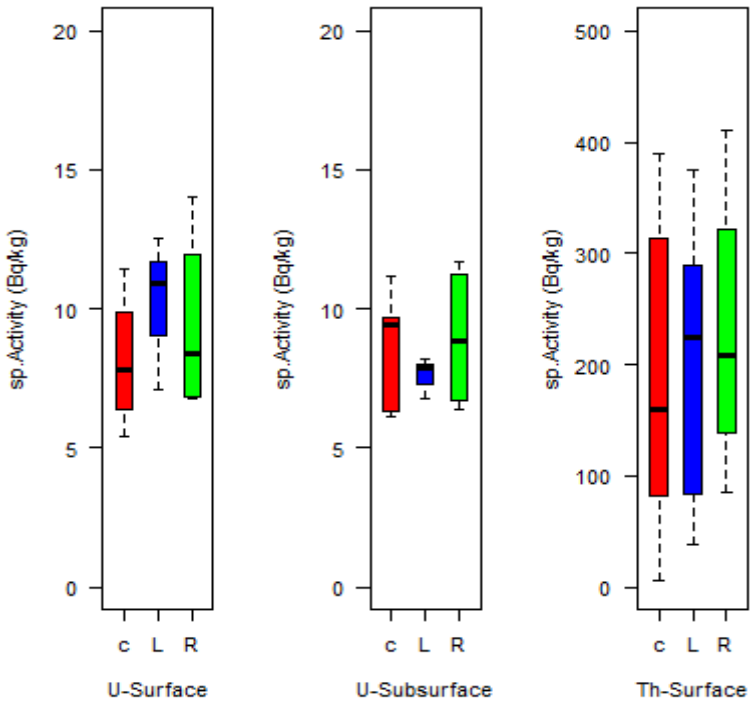

***Figure 4.5a*. Specific activities in river Tiva sands (L-left, C-center, R-right)**

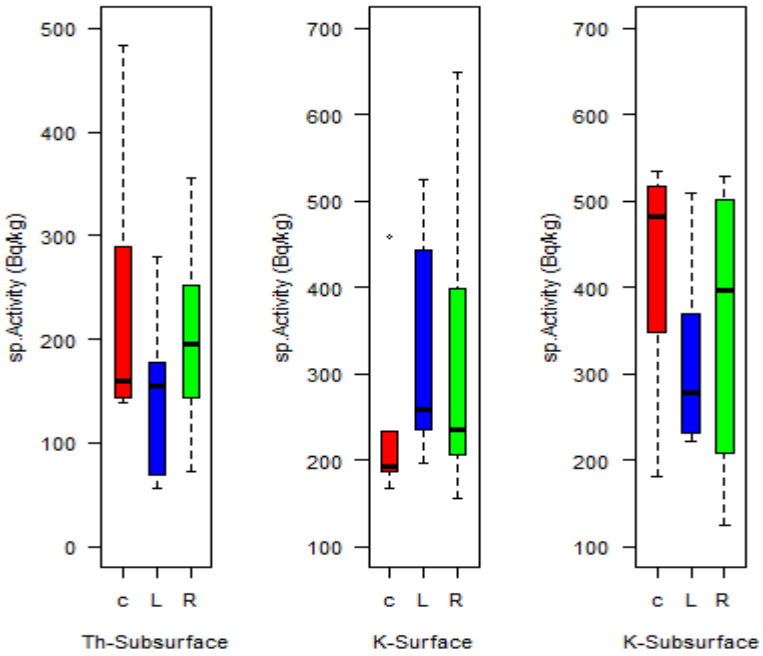

***Figure 4.5b*. Specific activities in river Tiva sands (L-left, C-center, R-right)**

Statistical values in table 4.8 for kurtosis and skewness coefficients are non-zero, indicating the non-existence of normal distributions. All of the radionuclides' distribution is Platykurtic i.e. they have a lower, wider peak around the mean and thinner tails hence are sub-Gaussian in distribution. However, the right tail is longer as compared to the left hence positive skewness. There is a strong positive correlation between ^{232}Th and ^{238}U in the heavy sands (R=0.68) which indicates the same origin but exist a weak positive correlation between ^{40}K and ^{232}Th (R=0.29) and ^{40}K and ^{238}U (R=0.25).

Table 4.8. **Summary statistics for radionuclide concentrations in river Tiva sands**

	^{238}U	^{232}Th	^{40}K
Kurtosis	-0.32	-0.76	-1.16
Skewness	0.55	0.58	0.43
Correl. (R)	^{232}Th/^{238}U=0.68	^{40}K/^{232}Th=0.29	^{40}K/^{238}U=0.25

Currently, river sands are used in building constructions and may be mined in future for industrial use, and therefore, the gamma-ray radiation hazards evaluated were Ra_{eq}, H_{ex} and Iγ and absorbed dose estimated. The respective calculated values were 319 Bq kg^{-1}, 0.86 and 2.27 for Ra_{eq}, H_{ex} and Iγ. The estimated absorbed dose (D) was 150 nGy h^{-1}.

Radium equivalent (Ra_{eq}) is almost 5.5 times that of Mwanyani limestone samples within the same County as indicated by Mulwa (2013) but below 370 Bq kg^{-1} the recommended value. Therefore, this value suggests that the sands pose no danger to the users or population living in the area. Another radiation hazard index that fits well with the recommendation is external hazard index (H_{ex}). It is well below the unity which is insignificant. However, the value is almost equal to one which suggests that there could be relatively high radiation exposure to the population, but will not have any deterministic effects. Having said that, a worrying factor is a representative level index (Iγ) which is more than double the recommended value of unity for it be insignificant. Iγ is more than one, suggesting that the radiation exposure to radioactivity is significant. The mean absorbed dose rate (D) obtained was almost 3 times the globally recommended value of 55 nGy h^{-1}. The reason why the representative level index and

the absorbed dose rate are well above the recommended values is attributed to the presence of monazites in the heavy sands and translate to an annual effective dose of 0.18 mSv yr^{-1}. However, this is more than the world-mean of 0.07 mSv yr^{-1} (Orgun, *et al*., 2007). These monazites explain the high ^{232}Th activity concentration.

4.3. Heavy Metals

4.3.1. Minimum detection limit

The minimum detection limit (MDL) for the concerned elements were obtained by analyzing the standard sample (River-clay IAEA-pt XRF-33). The minimum detection limit values were obtained as per the equation (4.1).

$$MDL = 3 \times \frac{C}{P}\sqrt{R_b} \quad \text{.....4.1}$$

where, R_b is the background area of the element, P is the peak area of the element, C is element's concentration in mg kg^{-1}.

Few of the experimental MDL values presented in table 4.9 were used to estimate the minimum detection limits for other elements as shown in figure 4.6.

Table 4.9. Experimental and estimated minimum detection limit values

Element	K	Ca	Ti	Mn	Fe	Zn	Rb	Sr	Y	Zr	Nb
Atomic No.	19	20	22	25	26	30	37	38	39	40	41
Exp. MDL (ppm)	387	220	91	50	37	17	10	10	10	8	11

The minimum detection limits in ppm for other elements of interest obtained by applying line equation of figure 4.6 were: V; 70, Cr; 58, Cu; 25, Zn; 21, Co; 34, Pb; 0.2, Ni; 29, As; 13.

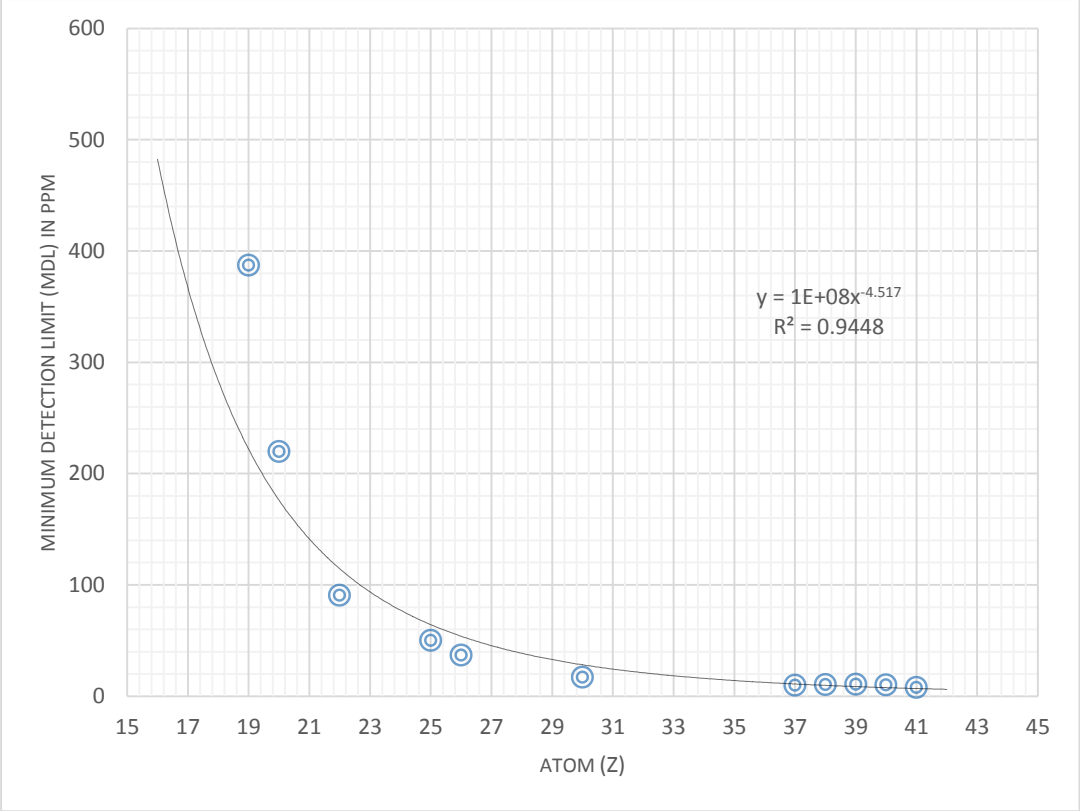

Figure 4.6. **Best-line fit for elements' minimum detection limits**

4.3.2. Quality assurance

River-clay (IAEA-pt XRF-33) were analyzed using EDX in order to validate the results obtained by using the same method to analyze heavy sands for heavy metals. Table 4.10 gives the comparison between the measured values and those of the certified values. The observed major deviations of Co and Cu could be as a result of k-beta lines of high occurring elements overlapping with k-alpha lines of the low occurring elements. In this case, k-beta lines of iron could explain the high deviation occurrence observed in cobalt.

4.3.3. Heavy metal analytical results

The concentrations and distributions of Fe, Ti, V, Mn, Cr, Cu, Zn, Co, Sr, Zr, Pb, Ni and As were investigated up to a depth of 1 m and their mean concentrations were used to calculate the level of pollution in river Mwita Syano sands. Table 4.11 and 4.12 shows the summarized results of metal concentrations in the sand samples. Their abundance in µg g^{-1} varied as: Fe> Ti > Mn > Sr > V > Zr > Cr > Co > Zn > Cu > Pb. The mean concentrations µg g^{-1} of side-river sands were much higher compared to those from floor of the river sand samples and varied as: Fe > Ti > V > Mn > Co > Zr > Sr>Cr

> Zn > Cu > Pb. The mean concentrations of nickel and arsenic were below their calculated minimum detection limits of 30 µg g^{-1} and 13 µg g^{-1} respectively in both side-river and river sand samples. Figures 4.7a through 4.8b shows metal concentration variations in both river and side-river sand samples.

Fe, Cu, Mn and Cr mean concentrations were comparable to the values obtained from Belgium north-sea and Scheldt region while those of Pb and Zn were less. However, V and Ti mean concentrations were higher (Van Alsenoy *et al.*, 1993). On the other side, the side-river sands mean concentrations were higher except for Pb and Zn. The mean metal concentrations were higher than those of Agbabu Bitumen deposits in Nigeria except for Zn which was comparable (Fagbote & Olanipekun, 2010). Sr and V mean concentrations were comparable to the metal concentrations for the red dunes of Bhimili of Visakhapatnam, India. Those of Co, Cr and Cu were higher while for Zn, Zr and Pb values were less as compared to the results from the same region (Rao *et al.*, 2013).

Enrichment factors (EFs) and Geo-accumulation indices ($I_{geo)}$ were applied in evaluating the extent to which heavy metals pollute sands. The respective values are tabulated in Table 4.13. The control sample was taken to be that of an average shale (the integrate crystal material derived from different earth-surface environments). Fe was used as the normalizing metal in the samples due to its low occurrence variability and its most abundance (Sutherland, 2000).

The mean concentration of 36203 $\pm$ 2353 µg g^{-1} for Fe was obtained with a relatively wide range of a maximum of 76000 µg g^{-1} and a minimum of 16125 µg g^{-1} (table 4.11). The mean concentration of 192385 $\pm$ 12467 µg g^{-1} was found for the side-river sand samples (table 4.12). The mean I_{geo} of -0.97 reveals that the sample fell in the class 0, which is unpolluted (table 4.13). Its EF of 1 indicates the deficiency to the minimal enrichment of Fe in the heavy sands. The two methods of checking the level of contamination agree well. However, the two methods differ slightly in the case of the side-river sands. The mean I_{geo} for the side-river sands is 1.44 implying a moderate pollution whereas EF remains unchanged. In this case, I_{geo} is the appropriate mode since it is not being affected by the used normalizing metal.

Table 4.10. **Measured and certified values of the reference sample.**

	K	Ca	Ti	Mn	Fe	Zn	Cu	Co
certified values (*μg g*$^{-1}$)	19500	13800	4300	1000	29700	96.1	20.1	12.5
measured values (*μg g*$^{-1}$)	19500	14000	4620	1170	30600	114	49.2	203
% dev.	0	1.4	7.4	17	3	18	144	1524

Table 4.11. **Summary statistics of metal concentrations in river Mwita Syano sands in μg g^{-1}**

	Fe	Ti	V	Mn	Cr	Cu	Zn	Co	Sr	Zr	Pb
min	16125	1550	54.9	409	179	33.8	23.3	102	265	100	0.77
max	76000	20438	988	1638	396	82	95.5	553	547	785	10.1
1st Qu.	26709	2880	112.5	646	219	41.95	42.05	165	317	150	2.44
range	59875	18888	933.1	1229	217	48.2	72.2	451	282	685	9.33
3rd Qu.	42563	8648	337	1005	296	56.65	57.75	314	377	279	4.57
median	30083	4463	205	810	258	50	45	193	346	194	3.52
mean	36203	6037	275	846	260	50	51	253	358	264	3.75
SE.mean	2553	751	36	50	10	2	3	22	11	30	0.5
CI.mean.0.95	5189	1527	75	103	20	4	6	45	23	62	0.68
std.dev	15106	4445	218	300	57	12	17	132	66	181	2
coef.var	0.42	0.74	0.80	0.36	0.22	0.29	0.34	0.52	0.19	0.69	0.53
kurtosis	0.37	1.44	1.44	0.29	-0.38	-0.09	-0.12	-0.15	0.85	1.40	1.17
skewness	1.04	1.38	1.38	0.67	0.60	0.77	0.87	1.02	1.16	1.57	1.01

Table 4.12. **Summary statistics of metal concentrations in Mwita Syano side-river sands in µg g^{-1}**

	Fe	Ti	V	Mn	Cr	Cu	Zn	Co	Sr	Zr	Pb
min	36042	3963	66	1425	288	62.6	42.2	277	348	223	4.85
max	342083	77417	5500	4621	536	243	417	4329	577	4204	55.8
1st Qu.	90698	27335	1607	2256	3698	77.9	105	775	385	116	13.5
range	306041	73454	5434	3196	248	180.4	374.8	4052	229	3981	50.95
3rd Qu.	297396	75198	5403	4484	4910	234	386	3492	472	3054	30
median	195708	54791	3746	3485	436	157	251	2077	417	2077	18.9
mean	192385	47740	3264	3254	424	155	240	2190	440	2145	24
SE.mean	71844	17488	1322	771	53	47	92	950	49	848	10
CI.mean.0.95	228642	55655	4207	2454	170	152	293	3024	156	2701	34
std.dev	143689	34976	2644	1542	107	95	184	1900	98	1697	21
coef.var	0.75	0.73	0.81	0.47	0.25	0.62	0.77	0.87	0.22	0.79	0.89

Table 4.13. **Enrichment factors (EFs) and Geo-accumulation indices (I_{geo}) of metals in river Mwita Syano sands**

	Fe	Ti	V	Mn	Cr	Cu	Zn	Co	Sr	Zr	Pb
EF	1	1.71	2.76	1.30	3.77	1.48	0.70	17.4	2.75	2.15	0.24
I_{geo}	-0.97	-0.19	0.50	-0.59	0.95	-0.40	-1.48	3.15	0.49	0.14	-3.00
EF*	1	2.55	6.16	0.94	1.16	0.85	0.62	28.3	0.63	3.29	0.30
I_{geo}*	1.44	2.79	4.07	1.35	1.65	1.20	0.75	6.26	0.79	3.16	-0.29

Parameters with an asterisk represent those from side-river sand samples

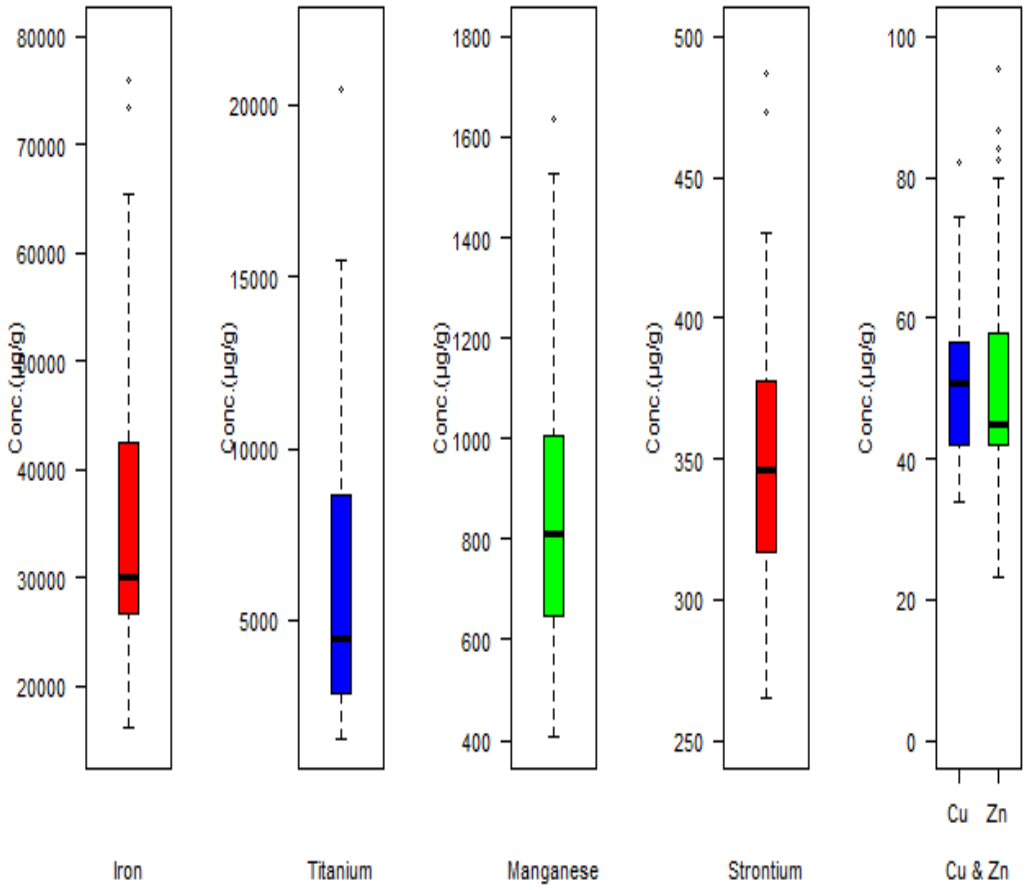

***Figure 4.7a*. Heavy metal concentrations variation in river Mwita Syano sands.**

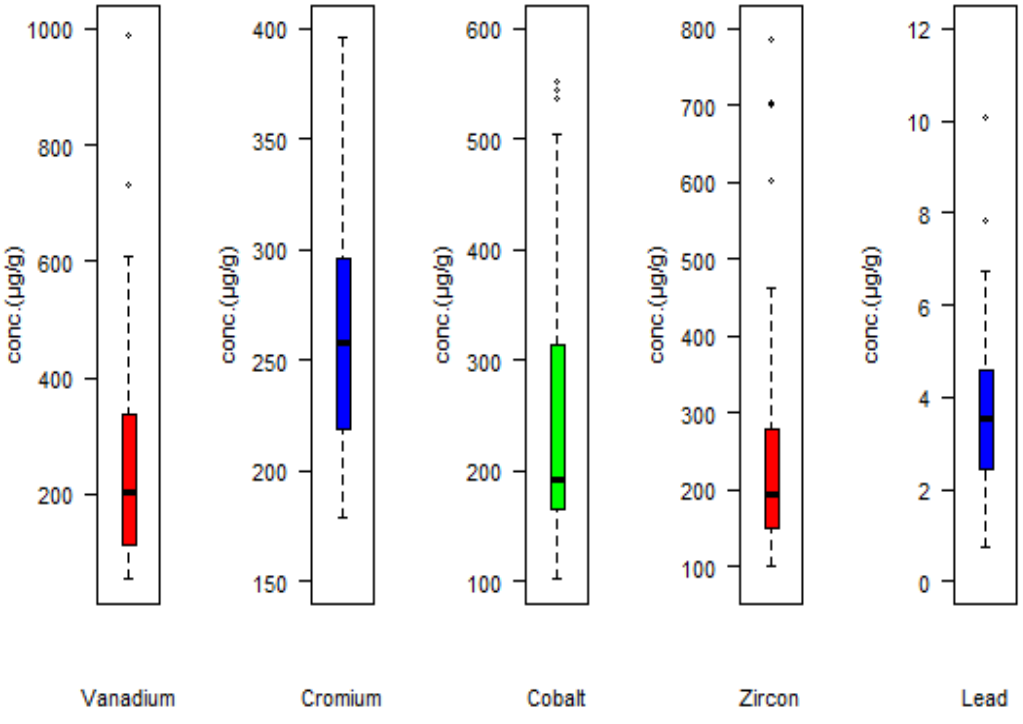

***Figure 4.7b*. Heavy metal concentrations variation in river Mwita Syano sands**

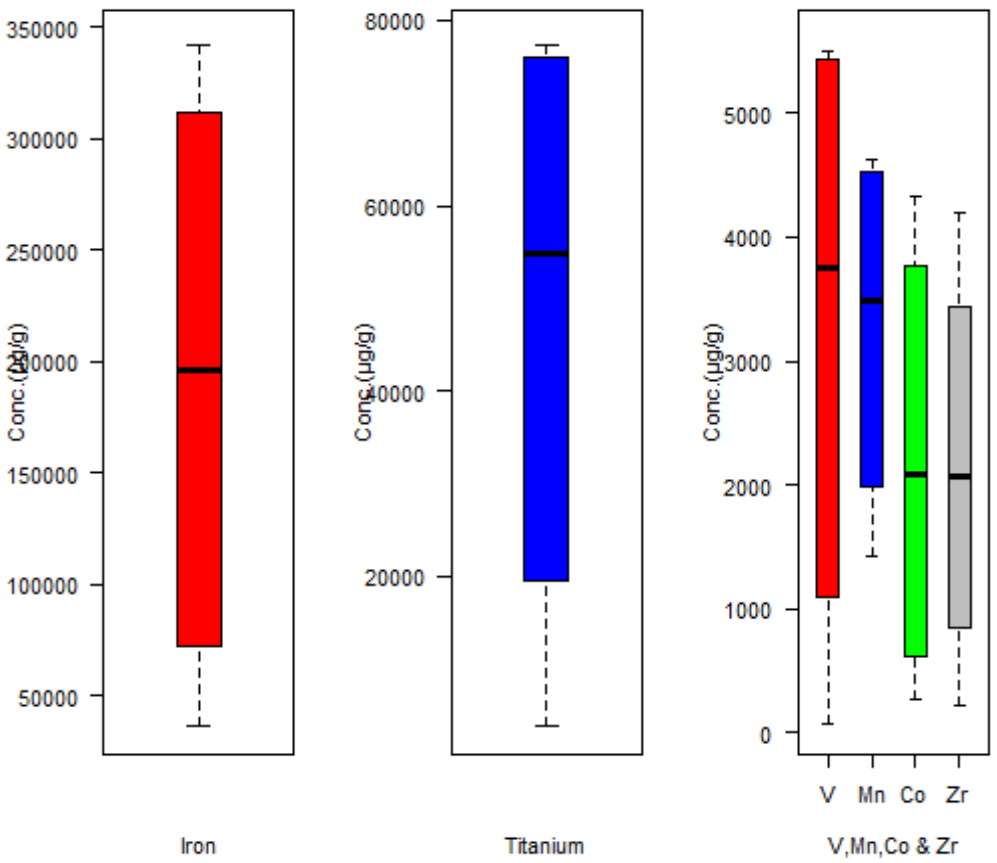

***Figure 4.8a*. Heavy metal concentrations variation in Mwita Syano side-river sands**

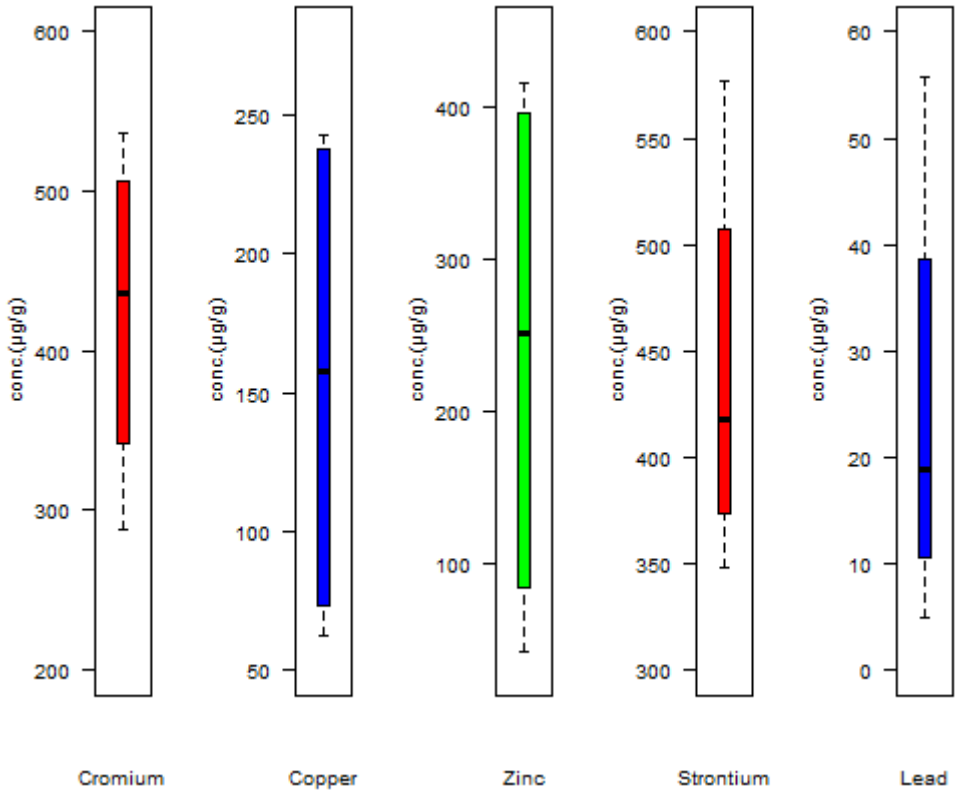

***Figure 4.8b*. Heavy metal concentrations variation in Mwita Syano side-river sands**

Titanium was found to have a mean concentration of 6037 ± 426 µg g^{-1} with a maximum of 20438 µg g^{-1} and a minimum of 1550 µg g^{-1} in the river sands (table 4.11) while the mean concentration of side-river sands was 47741 ± 3148 (table 4.12). The I_{geo} mean is -0.19 indicating unpolluted to moderately polluted river sands while that of side-river sands is 2.79 implying moderately to strongly pollution. EF for the same is 1.71 and 2.55 implying deficiency to minimal enrichment and moderate enrichment respectively (table 4.13).

The mean concentrations for vanadium (V), chromium (Cr) and zircon (Zr) in river sands were 275 ± 40 µg g^{-1}, 260 ± 45 µg g^{-1} and 264 ± 20 µg g^{-1} respectively (table 4.11). Their respective mean concentrations for the side-river samples were 3264 ± 338 µg g^{-1}, 424 ± 86 µg g^{-1} and 2145 ± 142 µg g^{-1} (table 4.12). The mean I_{geo} for the three metals were 0.5, 0.95 and 0.14 respectively all indicating unpolluted to moderately polluted. For the side-river samples, V, Cr, and Zr had I_{geo} of 4.07, 1.65 and 3.16 respectively implying side-river sands are strong to very strongly polluted with V, moderately polluted with Cr and strongly polluted with Zr. The respective EF values for V, Cr and Zr in the river sands were 2.76, 3.77 and 2.15 indicating moderate enrichment. On the hand, their respective EF values in the side-river sands were 6.16, 1.16 and 3.25 (table 4.13). This shows that the side-river sands are significantly enriched with V, deficiency to the minimal enriched with Cr and that of Zr remained unchanged as in the river sands.

For manganese (Mn), cobalt (Co) and strontium (Sr), mean concentrations of 846 ± 74 µg g^{-1}, 253 ± 30 µg g^{-1} and 358 ± 25 µg g^{-1} were found (table 4.11) in river sands while that of side-river samples were 3254 ± 234 µg g^{-1}, 2190 ± 181 µg g^{-1} and 440 ± 34 µg g^{-1} respectively (table 4.12). Mean I_{geo} for Mn, Co and Sr were -1.59, 3.14 and 0.49 implying river sands are unpolluted with Mn, strongly polluted with Co, and unpolluted to moderately polluted with Sr. I_{geo} for the side-river sands were 1.35, 6.26 and 0.79 for Mn, Co and Sr respectively showing an increase of Mn pollution to that of moderately polluted, Co is alleviated to that of very strongly polluted while Sr remained unchanged. The respective EF values were 1.30, 17.4 and 2.75 indicating deficiency to minimal enrichment, significant enrichment, and moderate enrichment in that order. The side-river sand samples had EF values of 0.94, 28.3 and 0.63 for Mn, Co and Sr respectively

which translates to deficiency to minimal enrichment for Mn and Sr while Co is very high enrichment (table 4.13).

The mean concentrations of Cu, Zn and Pb in river sands were 51 ± 8 μg g^{-1}, 51 ± 9 μg g^{-1}, 3.75 ± 0.33 μg g^{-1} respectively (table 4.11). On the other hand, their respective mean concentration was 155 ± 19 μg g^{-1}, 240 ± 29 μg g^{-1} and 24.6 ± 4 μg g^{-1} in the side-river sands (table 4.12). The mean I_{geo} of Cu, Zn and Pb were -0.40, -1.48 and -3.0 implying that the river sands are unpolluted with Cu, Zn and Pb respectively. That of the side-river sands recorded an I_{geo} value of 1.20, 0.75 and -0.29 for Cu, Zn and Pb respectively. The side-river sands were moderately polluted with Cu and unpolluted to moderately polluted with Zn and Pb. The corresponding EF values for Cu, Zn and Pb were 1.48, 0.70 and 0.24 in the river sands and 0.85, 0.62 and 0.30 in the side-river sands implying the deficiency to minimal enrichment of Cu, Zn and Pb for both samples.

Generally, the side-river sand samples exhibited high metal concentrations for all the metals of interest as compared to river sand samples. There was no significant difference in metal concentration means between the side-river sands and the river sands as depicted by the p-values of 0.4 for EF at 95 % confidence interval level. The river-side samples were more enriched with and polluted with metals as alluded by enrichment factors and geo-accumulation indices. However, there was a significant difference between the enrichment factor method and geo-accumulation index method measuring the level of heavy metals contamination as suggested by the p-values of 0.004 at 95% confidence level based on paired t-test and 0.028 at 95 % confidence level on a random t-test (Welch t-test). The cause of difference could be attributed to the fact that EF is dependent of normalizing metal whose occurrence in the concerned environment could be alleviated to high levels that may undermine entire measurement of heavy metals contamination. Another shortcoming that undermines EF is its inability to measure the contamination of the environment with the metal taken as the normalizing element.

4.3.4. Depth profile and distribution along the river

Metal concentration variations according to depth are presented in figures 4.9a to 4.9d. Many metals were more concentrated at the sub-surface samples with exceptions of Sr and Pb whose concentrations at the sub-surface were less than both the surface and 1-

meter deep samples. This could be attributed to the sediment properties as well as metals response to agents of transport in the medium. Furthermore, it could suggest that heavy metals get carried more easily on the surface as compared to the sub-surface sample. Since the sands are always deposited, the surface and sub-surface ratio suggest that the sands have no anthropogenic inputs. It was also observed that metal concentrations of side-river samples were higher than those obtained from the river sands. It proves that metals get easily deposited when water velocity is low as compared with when the velocity of transporting medium is high.

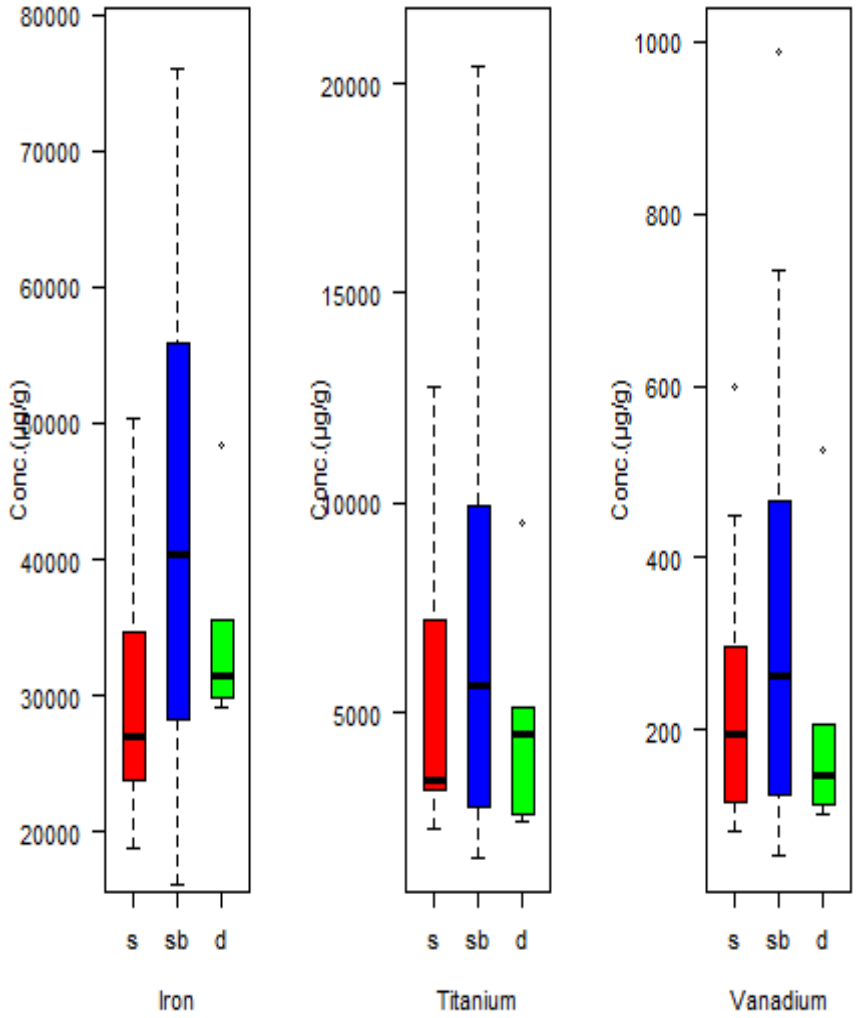

***Figure 4.9a*. Fe, Ti, V concentrations variation (s=surface, sb=subsurface, d≈1 m deep)**

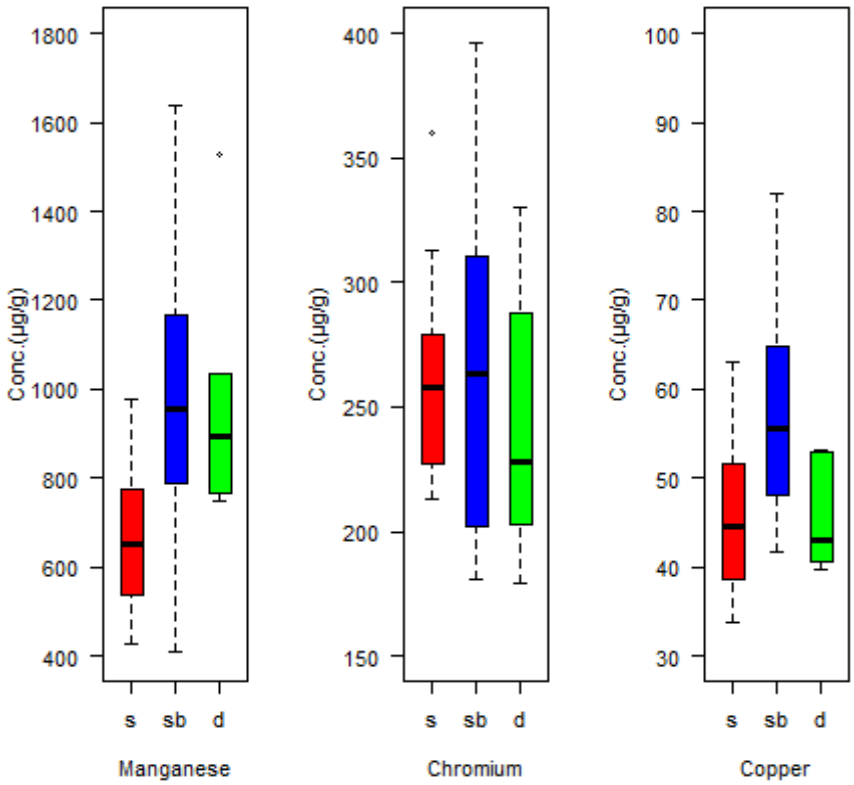

***Figure 4.9b*. Mn, Cr, Cu concentrations variation (s=surface, sb=subsurface, d≈ 1 *m* deep)**

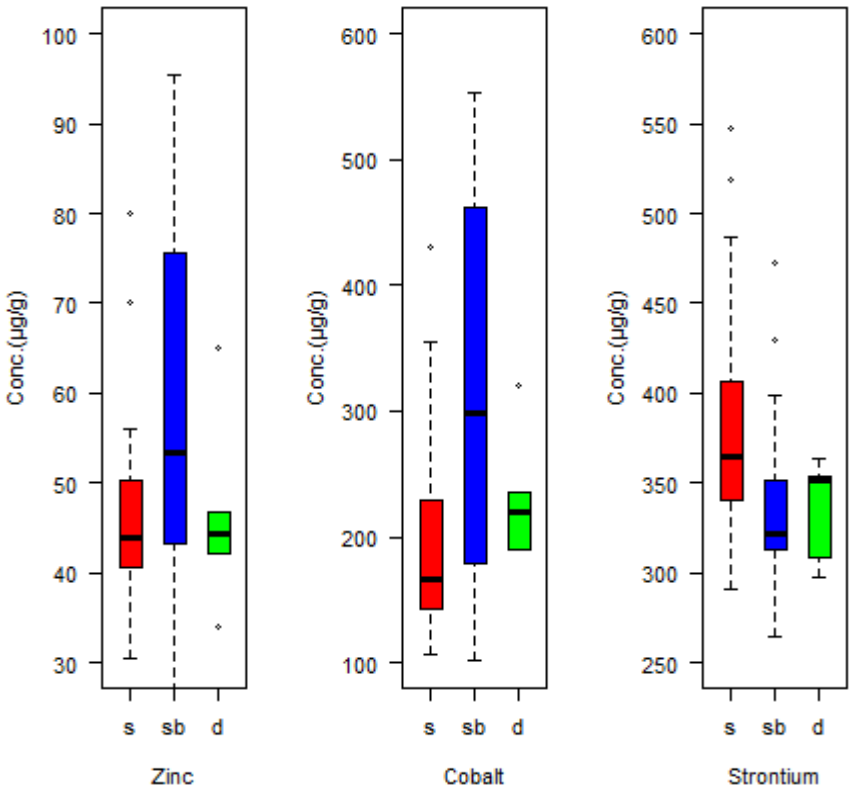

***Figure 4.9c*. Zn, Co, Sr concentrations variation (s=surface, sb=subsurface, d≈ 1 *m* deep)**

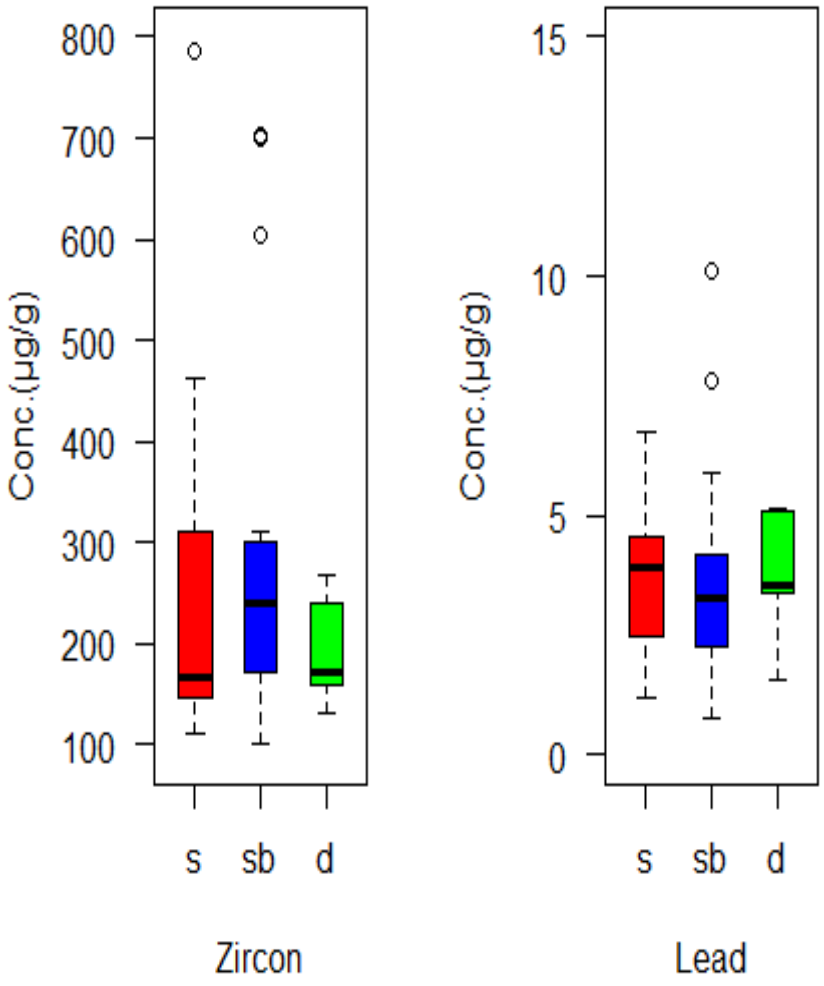

Figure 4.9d. **Zr and Pb concentrations variation (s=surface, sb=subsurface, d≈ 1 m deep)**

The metal concentrations were evenly distributed along the river Mwita Syano for all metals (figure 4.10). It was observed that there was a spatial site variation of heavy metal concentrations. Site 4 had the lowest amount of most metals. This could be due to the high river gradient at that section. On the other hand, site 5 contained almost the highest amount of most metals which could be indicating a gentle slope of the river in that section. The trend line can be an indicator of river slopeness and breath. A steep and narrower river sections are more likely to record the lowest metal concentrations and vice-versa.

***Figure 4.10*. Distributional trend of metals in sampled sites along river Mwita Syano**

4.3.5. Correlation analysis

Heavy metals with an exception of Cr, Cu, Zn and Co have positive kurtosis indicating a more peaked distribution while all the heavy metals were positively skewed (table 4.11). There are very strong positive relationships between Fe and Ti, V, Zn, Cu, Mn, Co and Zr (table 4.14) implying the same source of origin. The same can be said between Ti and Zn, V, Co and Zr. Also, V relates strongly with Zn, Co and Zr perhaps indicating the same source of origin. Mn correlates well with Cu and Co. Furthermore, Zn relates positively strong with Zr and Co. Lastly Co and Zr may share the same origin because they relate well. The combinations that have moderate relationship are: (1) Fe and Pb, (2) Ti and Mn, Cr, Cu, (3) V and Mn, Cu, (4) Mn and Zn, Zr, (5) Cr and Cu, Zn, Co, (6) Cu and Zr, (7) Sr and Zr. Moderate relationship suggests that the elements may have been affected differently by factors of sand formation as well as response differently to agents of leaching and transport mechanism. Sr relates poorly to all other metal elements suggesting different parent material from the rest or has suffered a lot since formation due to agents of transport.

Table 4.14. **Correlation coefficient matrix for metals in sands excluding those from the side-river sands**

	Fe	**Ti**	**V**	**Mn**	**Cr**	**Cu**	**Zn**	**Co**	**Sr**	**Zr**	**Pb**
Fe	1										
Ti	0.94	1									
V	0.92	0.98	1								
Mn	0.68	0.51	0.47	1							
Cr	0.34	0.31	0.28	0.11	1						
Cu	0.70	0.59	0.54	0.72	0.34	1					
Zn	0.91	0.87	0.84	0.56	0.46	0.67	1				
Co	0.96	0.90	0.86	0.65	0.38	0.75	0.84	1			
Sr	-0.01	0.13	0.08	0.07	-0.19	0.19	0.06	0.03	1		
Zr	0.83	0.92	0.89	0.47	0.19	0.56	0.81	0.80	0.39	1	
Pb	0.56	0.57	0.54	0.34	-0.03	0.38	0.50	0.54	0.15	0.58	1

4.3.6. Heavy metals summary outline

The mean metal concentrations of thirteen elements were investigated with an aim of gauging the extent at which they have polluted the sands or could their presence in anomalous amount be an indication of associated mineral ores within the region. Iron was present in a high amount which could be an accessory to minerals and same can be said for Titanium. The sands were found to be mostly unpolluted of metals to moderate polluted based on geo-accumulation indices values and deficiency to a minimum deficiency on enrichment factor scale. Enrichment factor suggests the source of enrichment to be of geogenic origin except for Cr and Co which suggest otherwise.

Table 4.15. **Summary outline of metal pollution of river Mwita Syano sands**

Metal element	**EF values [] and their implications**		**Geo-accumulation indices [] and their implications**	
	River sands	Side-river sands	River sands	Side-river sands
Fe	[1]Def.-Min.	[1]Def.-Min.	[-0.97]Unpol.	[1.44]Mod.
Ti	[1.71]Def.-Min	[2.55]Mod.	[-0.19]Unpol.-Mod	[2.79]Mod-Str.
V	[2.76]Mod.	[6.16]Sign.	[0.50]Unpol.-Mod	[4.07]Str.-V.Str.
Mn	[1.30]Def.-Min	[0.94]Def.-Min.	[-0.59]Unpol.	[1.35]Mod.
Cr	[3.77]Mod.	[1.16]Def.-Min.	[0.95]Unpol.-Mod	[1.65]Mod.
Zr	[2.25]Mod.	[3.29]Mod.	[0.14]Unpol.-Mod	[3.16]Str.
Co	[17.4]Sign.	[28.3]V. high	[3.15]Str.	[6.26]V. Str.
Cu	[1.48]Def.-Min.	[0.85]Def.-Min.	[-0.40]Unpol.	[1.20]Mod.
Zn	[0.70]Def.-Min.	[0.62]Def.-Min.	[-1.48]Unpol.	[0.75]Unpol.-Mod.
Sr	[2.75]Mod.	[0.63]Def.-Min.	[0.49]Unpol.-Mod	[0.79]Unpol.-Mod
Pb	[0.24]Def.-Min.	[0.30]Def.-Min.	[-3.0]Unpol.	[-0.29]Unpol.

Key Definitions

Def.-Deficiency, Min.-Minimum, Mod.-Moderate, Unpol.-Unpolluted, Sign.-Significant, V. high-Very high, Str.-Strongly, V. Str.-Very Strong.

CHAPTER FIVE

CONCLUSIONS AND RECOMMENDATIONS

5.1. Conclusions

The XRD analysis of heavy sand samples from river Mwita Syano indicates the presence of minerals such albite (21.4 %), hornblende (14.9 %), ilmenite (3.9 %), magnetite (1.9 %), diopside (3.5 %), microcline (1.4 %), orthoclase (1.1 %) and quartz (52.7 %). Because of incomplete quantitative analysis and lack of information on the cost of mineral separation, the economic importance of the mineral sands in the heavy sands from river Mwita Syano is uncertain.

The primordial radioactivity mean for ^{232}Th, ^{238}U and that of ^{40}K in heavy sands were 199 Bq kg^{-1}, 8.8 Bq kg^{-1} and 329 Bq kg^{-1} respectively. ^{40}K accounted for 61 % while ^{232}Th gave 37 % and the rest 2 % was from ^{238}U of the total primordial radioactivity. ^{238}U and ^{40}K radiation are within the accepted limits of 50 Bq kg^{-1} and 500 Bq kg^{-1} respectively. That of ^{232}Th activity is almost 4 times more than the accepted limits of 50 Bq kg^{-1}. The radiation hazard indices signify that the natural radioactivity poses no danger to the population living in the area. The mean total gamma absorbed dose rate calculated from of ^{232}Th, ^{238}U and ^{40}K concentrations in river Tiva heavy sands was 150 nGy h^{-1}. This yielded an annual effective dose of 0.18 mSv yr^{-1} which is within the internationally accepted limit of 1 mSv yr^{-1} but well above the world's average of 0.07 mSv yr^{-1}.

The mean concentrations of eleven heavy metals (Fe, Ti, V, Mn, Cr, Co, Cu, Zn, Sr, Zr, Pb) were evaluated and found to be higher than the values recommended in Consensus-Based Sediment Quality Guidelines of Wisconsin (CBSQG) except for Zn and Pb (appendix table 7). Also, the mean concentrations values were higher than those of average shale except for Fe, Zn and Pb (appendix table 4). Ni and As mean concentrations were below the minimum detection limit. The extent to which the sediments are contaminated was based on enrichment factor (EF) and geo-accumulation index (I_{geo}) evaluation. EF of Fe (1), Ti (1.71), Mn (1.30), Cu (1.48), Zn (0.7) and Pb (0.24) shows deficiency to minimal enrichment while river sands were moderately enriched by V (2.76), Cr (3.77), Sr (2.75) and Zr (2.15). There is the significant enrichment of Co (17.36). This depicts the source of heavy metals in

rivers in this region as natural. The mean I_{geo} indices for Mn, Zn, Fe, Ti, Cu and Pb indicates that the river sands are unpolluted of these elements. The river sands were unpolluted to moderately polluted by V, Cr, Sr and Zr while strongly polluted by Co as the indicated by their I_{geo} indices.

5.2. Recommendations

- Accurate quantitative mineral analysis of heavy mineral concentrate speciation is required as part of prospection of mineral sand deposits.
- Radioactivity investigation of the surrounding environment is required so as to gauge the radiological risk exposure to the general public.
- Radiological study of water from these rivers should be done to gauge the ingested radiation by either drinking or through cooked food.
- The geochemistry study of the surrounding environment should be done to pinpoint the source of metals anomalies which are crucial in searching for new minerals deposits.

REFERENCES

Abdi, M. R., Faghihian, H., Kamali, M., Mostajaboddavati, M., & Hasanzadeh, A. (2006). **Distribution of natural radionuclides on coasts of Bushehr Persian gulf, Iran**. *Iranian Journal of Science & Technology, Trans. A, 30*(3), 259-269.

Akinmosin, A., Osinowo, O. O., & Oladunjoye, M. A. (2009). **Radiogenic components of the Nigeria tarsand deposits**. *Earth Sci. Res. J., 1*(13), 64-73.

Akpon, I. O., & Thompson, E. A. (2013). **Assessment of heavy metal contamination of sediments along the cross river channel in Cross River state, Nigeria**. *IOSR Journal of Environmental Science, Toxicology and Technology, 2*(5), 20-28.

Ali, M. A., Krishnan, S., & Banerjee, D. C. (2001). **Beach and inland heavy mineral sand investigations and deposits in India – An overview**. *Expl. Res. Atomic Mins.*, 13.

Al-Sulaiti, H. A. (2011). ***Determination of natural radioactivity levels in the state of qatar using high-resolution gamma-ray spectrometry***. Faculty of Engineering and Physical Sciences, University of Surrey, Department of Physics, Guildford.

Anderson, J. F. (2011). ***Investigation of sand resources in North Dakota: Sedimentological characterization of surficial sand deposits for potential use as proppant***. Department of Minerals Resource, North Dakota.

ARPANSA. (2008). ***Radiation exposure in the transport of heavy mineral sands***.

Begum, A., HariKrishna, S., & Khan, I. (2009). **Analysis of heavy metals in water, sediments and fish samples of Madivala lakes of Bangalore, Karnataka.** *International Journal of ChemTech Research*, 245-249.

Beretka, J., & Mathew, P. J. (1985). **Natural radioactivity of Australian building materials, industrial wastes and by-products**. *Health Phys, 48*, 87-95.

Carlos, A. H., Alicia, F. C., & Luisa, M. P. (2014). **Heavy metal accumulation in leaves of aquatic plant Stuckenia filiformis and its relationship with sediment and water in the Suquía river (Argentina)**. *Microchemical Journal, 114*, 111-118.

Chadima, S. A., McCormick, K. A., Schulz, L. D., & Haggar, T. N. (2003). ***X-ray diffraction analysis of post-cretaceous sand and gravel units in southeastern South Dakota***. University of South Dakota, Environment and Natural Resources.

Chandra, R., Bharagava, R. N., yadav, S., & Mohan, D. (2009). **Accumulation and distribution of toxic metals in wheat (Triticum aestivum L.) and Indian mustard (Brassica campestris L.) irrigated with distillery and tannery effluents**. *Journal of Hazardous Materials, 162*, 1514-1521.

Cook, J. D. (1969). ***Heavy minerals in Alaskan beach sand deposits***. The University of Alaska College, Mineral Industry Research Laboratory.

Corbell, M. C. (2004). ***Application of x-ray diffraction in conservation science and archaeometry***. Canadian Conservation Institute, Ottawa, Canada.

Currie, L. A. (1968). **Limits for Qualitative Detection and Quantative Determination.** *Analytical Chemistry, 40*(33), p. 586.

Deng, Y., White, G. N., & Dixon, J. B. (2009). ***Soil mineralogy laboratory manual.*** Texas A&M University, College Station, Soil and Crop Sciences. Texas: Authors.

Dodson, R. G. (1953). ***Geology of the North Kitui.*** Geol. Surv. Kenya.

Duruibe, J. O., Ogwuegbu, M. O., & Egwurugwu, J. (2007). **Heavy metal pollution and human biotoxic effects.** *International Journal of Physical Sciences, 2*(5), 112-118.

Eisenbud, M., & Gesell, T. (1997). ***Environmental radioactivity*** **(4th ed.)**. London: Academic Press.

El-Kameesy, S. U., El-Ghany, S. A., El-Minyawi, S. M., Miligy, Z., & El-Mabrouk, E. M. (2008). **Natural radioactivity of beach sand samples in the Tripoli region, northwest Libya**. *Turkish J. Eng. Env. Sci., 32*, 245-251.

Elsner, H. (2010). ***Heavy minerals of economic importance; assessment manual***.

Eunice, E. U., Duru, C. B., & Fabian, O. (2013). **XRD characterization of sand deposit in river Niger (South Eastern Nigeria)**. *American Chemical Science Journal, 3*(3), 287-293.

Fagbote, E. O., & Olanipekun, E. O. (2010). **Evaluation of the status of heavy metal pollution of sediment of Agbabu bitumen deposit area, Nigeria**. *European Journal of Scientific Research, 41*(3), 373-382.

Fitzpatrick, M. E., Fry, A. T., Holdway, P., Kandil, F. A., Shackleton, J., & Suominen, L. (2005). ***Determination of residual stresses by x-ray diffraction***. Measurement Good Practice Guide No. 52, National Physical Laboratory.

Focazio, M. J., Szabo, Z., Kraemer, T. F., Mullin, A. H., Barringer, T. H., & DePaul, V. T. (1998). ***The occurrence of selected radionuclides in ground water used for drinking water in the United States: A targeted reconnaissance survey.*** Water-Resources Investigation, U.S Geology Survey.

Galas-Gorchers, H. (1991). **Dietary intake of patricide residues; cadmium, mercury and lead.** *Food add., 8,* 793-800.

Gesell, T. F., & Prichard, H. M. (1975). **The technologically enhanced natural radiation environmental.** *Health Physics, 28,* 361-366.

Gindy, A. R. (1961). **Radioactivity in monazite, zircon and 'radioactive black' grains in blacksands of Rosetta**. *Egypt, Econ. Geol., 56,* 436-441.

GMP. (2011). ***African minerals sands***.

Hamby, D. M., & Tynybekov, A. K. (2002). **Uranium, thorium, and potassium in soils along the shore of lake Issyk-Kyol in the Kyrghyz Republic**. *Env. Monit. Assess, 73,* 101-108.

Holum, J. R. (1983). ***Elements of general and biological chemistry,* (6th ed.)**. N.Y: John Wiley and Sons.

Huu, H. H., Rudy, S., & Damme, A. V. (2010). **Distribution and contamination status of heavy metals in estuarine sediments near Cau Ong Harbor, Ha Long Bay, Vietnam**. *Geology Belgica, 13*(1-2), 37-47.

IAEA. (2003). ***Collection and preparation of bottom sediment samples for analysis of radionuclides and trace elements***. VIENNA: IAEA in Austria.

ILUKA. (2008). ***Mineral sands: An overview of the industry.*** Iluka Resources Limited, Geology.

Jenkin, R. (2000). **X-ray techniques: Overview. in R. A. Meyers, "*Encyclopedia of analytical chemistry"*** (pp. 13269-13288). Chichester: Ó John Wiley & Sons Ltd.

Joshua, E. O., & Oyebanjo, O. A. (2009). **Distribution of heavy minerals in sediments of Osun river basin southwestern Nigeria**. *Research Journal of Earth Sciences, 1*(2), 74-80.

Kabata-Pendis, A., & Mukherjee, A. B. (2007). **Trace elements from soil to human**.

Kamau, M. N. (2013). ***Characterization of soil mineralogy in relation to soil fertility functional properties for selected countries in Africa.*** Kenyatta University, Agricultural resource management.

Kannan, V., Rajan, M. P., Iyengar, M. A., & Ramesh, R. (2002). **Distribution of natural and anthropogenic radionuclides in soil and beach sand samples of Kalpakkam (India) using hyper pure germanium (HPGe) gamma ray spectrometry**. *Applied Radiation and Isotopes, 57*, 109-119.

Kitheka, U. J., Muluvi, g., Mathu, E., Mithya, J., Otieno, H., & Mutiso, F. (2011). ***Study report for the proposed water harvesting and utilization project at the South Eastern Kenya University (SEKU), kitui.***

Kumar, A., Kumar, M., Singh, B., & Singh, S. (2003). **Natural activities of uranium-238, thorium-232 and potassium-40 in some Indian buildings materials**. *Radiation Measurements, 36*(1-6), 465-469.

Luigi, B., Maurizio, B., Giorgio, M., Renato, M., & Serena, R. (2000). **Radioactivity in raw materials and end products in the Italian ceramics industry**. *Journal of Environmental Radioactivity, 47*, 171-181.

Macdonald, E. H. (1983). ***Alluvial mining. The geology, technology and economics of placers.*** London: New York (Chapman and Hall).

Malanca, A., Repetti, M., & Gazzola, A. (1995). **A radiological investigation on the monazite sands of the Atlantic Brazilian shore**. *Nucl. Geophys., 9*, 453-459.

Marathe, R. (2012). **XRD and SEM analysis of Tapti river sediment: A case study.** *Archives of Applied Science Research, 4*(1), 78-84.

Mathu, E. M. (1992). ***The Mutito and Ikoo faults in the Pan-African Mozambique belt, Eastern Kenya***. Netherlands: Kluver Academic Publishers.

Mathu, E. M., & Tole, M. P. (1984). **Geology of the Ithinga hills area.** *Journ. afri. Earth Sci., 2*, 1-16.

MDP. (2001). ***Mineral data publishing.*** **version 1.2.**

Mediolla, L. L., Domingues, M. C., & Sandoval, M. R. (2008). **Environmental assessment of and active tailings pile in the State of Mexico (Central Mexico)**. *Research Journal of Environmental Sciences, 2*(3), 197-208.

Meyer, R. A. (2000). ***Encyclopedia of analytical chemistry -x-ray techniques: Overview***. Ó John Wiley & Sons Ltd.

Ministry of Environment and Mineral Resources. (2012). ***National Environment Policy***. Nairobi, Kenya.

Mirjana, B. R., Saeed, M. A., Velibor, B. A., & Scepan, S. M. (2009). **Radioactivity of sand from several renowned public beaches and assessment of the corresponding environmental risks**. *journal of the Serbian chemical society, 74*(4), 461-470.

Mitchell, S., & Perez-Ramirez, J. (n.d.). ***Surface science and methods in catalysis, 529-OO611-OOL x-ray diffraction.*** Institute for Chemical and Bioengineering, Switzerland.

Mulwa, B. M., Maina, D. M., & Patel, J. P. (2013). **Radiological analysis of suitability of Kitui South limestone for use as building material**. *International Journal of Fundamental Physical Sciences, 3*(2), 32-35.

Nolan, K. (2003). **Copper toxicity syndrome**. *J. Orthomol. Psychiatry, 12*(4), 270-282.

Nyamai, C. M., Mathu, E. M., Opiyo-Akech, N., & Wallbrecher, E. (2003). **A reappraisal of the geology, geochemistry, structures and tectonics of the Mozambique belt in Kenya, east of the rift system**. *African Journal of Science and Technology, 4*(2), 51-71.

Nyamai, C. M., Opiyo-Akech, N., Gaciri, S. J., & Fujimaki, H. (1999). **Geochemistry and tectonomagmatic affinities of the Mozambique belt intrusive rocks in Matuu-Masinga area, Central Kenya**. *Gondwana Res, 2*(3), 387-399.

Omar, M., & Hassan, A. (2002). **The occurrence of high concentration of natural radionuclides in black sands of Malaysian beaches**. *Jurnal Sains Nuklear Malaysia, 20*(1&2), 30-36.

Ong'olo, D. O. (2001). ***International investment and environmental issues: The case of Kenya's Kwale mineral sands project.***

Orgun, Y., Altinsoy, N., Sahin, S. Y., Gungor, Y., Gultekin, A. H., Karaham, G., & Karaak, Z. (2007). **Natural and anthropogenic radionuclides in rocks and beach sands from Ezineregion (Canakkale), Western Anatolia, Turkey**. *Applied Radiation and Isotopes, 65*, 739-747.

Orth, R. A., & Wells, D. V. (2009). ***Sedimentation analysis of New Germany Lake, coastal and estuarine.*** Geology No. 10, Natural Resources, Maryland.

Osoro, M. K., Rathore, V. S., Mangala, M. J., & Mustapha, A. O. (2011). **Radioactivity in surface soils around the proposed sites for titanium mining project in Kenya**. *Journal of Environmental Protection, 2*, 460-464.

Palmer, B. M., & McInerney, J. J. (1994). **Optimization of energy window limits for photopeak detection system.** *Applied Radiation and Isotopes, 45*, 5-9.

Parnell, J. (2003). ***Mineral radioactivity in sands as a mechanism for fixation of organic carbon on the early Earth***. Department of Geology and Petroleum Geology, University of Aberdeen,.

Pauw, W., Mutiso, S., Mutiso, G., Manzi, H. K., Lasage, R., & Aerts, J. C. (2008). ***An assessment of the social and economic effects of the Kitui sand dams***. Nairobi, Kenya.

Prasong, K., Supphawut, B., & Succhin, U. (2007). **Distribution of natural radionuclides in Songkhla beach sands.** *Journal of Kasetsart, 41*(National Science), 157-164.

Praveena, S. M., Radojevie, M., Abdullahi, M. H., & Avis, A. Z. (2007). **Factor – cluster analysis and enrichment study of mangrove sediments – An example from Mengkabong Sabali**. *The Malaysian Journal of Analytical Science, 2*(2), 421-430.

Rao, P. S., Sujatha, B., Lakshminarayana, K., & Ratnam, S. V. (2013). **An assessment of heavy metals in red sand dunes near Bhimili of Visakhapatnam**. *Archives of Applied Science Research, 5*(1), 251-258.

Reguigui, N. (2006). ***Gamma ray spectrometry-practical information.***

RIVM. (1990). ***Measurements of the natural radioactivity of mineral sands***. RIVM Report No. 240801001, Bilthoven, Netherland.

Routray, S., & Rao, R. B. (2011). **Beneficiation and characterization of detrital zircons from beach sand and red sediments in India**. *Journal of Minerals & Materials Characterization & Engineering, 10*(15), 1409-1428.

Suryanarayana, C., & Norton, M. G. (1998). **X-ray diffraction, a practical approach**. In C. Hammond, *The basics of crystallography and diffraction* (2nd ed., pp. 207-221). OUP.

Sutherland, R. A. (2000). **Bed sediment associated trace metals in an urban stream, Oahu, Hawaii.** *Environmental Geology, 39*, 611-637.

Tijani, M. N., & Onodera, S. (2009). **Hydrogeochemical assessment of metals contamination in an urban drainage system: A case study of Osogbo township, SW-Nigeria**. *J. Water Resource and Protection, 3*, 164-173.

Titanium base. (2015, June 30th). **Retrieved from http://basetitanium.com/kwale-project/project-overview**

Tyler, R. M., & Minnitt, R. C. (2004). **A review of Sub-Saharan heavy mineral sand deposits: Implications for new projects in southern Africa**. *The Journal of The South Africa Institute of Mining and Metallurgy*, 89-100.

UNSCEAR. (1982). ***Ionising radiation: Sources and biological effect united nations scientific committee on the effect of atomic radiation.*** New York: United Nations. ISBN: 9211422426.

UNSCEAR. (1988). ***Sources and effects of ionizing radiation***. New York: United Nations.

UNSCEAR. (2000). ***Effects of atomic radiation to the general assembly, in united nations scientific committee on the effect of atomic radiation***. New York: United Nations.

Van Alsenoy, V., Bernard, P., & Van Grieken, R. (1993). **Elemental concentrations and heavy metal pollution in sediments and suspended matter from the Belgian North Sea and the Scheldt estuary.** *The Science of the Total Environment*, 153-181.

Varsha, M., Nidhi, M., Anurag, M., Singh, R. B., & Sanjay, M. (2010). **Effect of toxic metals on human health.** *The Open Nutraceuticals Journal, 3*, 94-99.

Vries, W., Romkens, P. F., & Schutz, G. (2007). **Critical soil concentrations of cadmium, lead and mercury in view of health effect on humans and animals**. *Reviews of Environmental Contamination and Toxicology, 191*, 91-130.

WHO. (2007). ***Health risks of heavy metals from long-range transboundary air pollution***.

APPENDICES

Appendix 1. Instrument and Materials

1.1 Equipment

i. A D2 Phaser Diffractometer
ii. McCrone micronizing mill
iii. Weighing balance
iv. Centrifuge
v. Vortex mixer

1.2 Materials

i. Standard reference material (Quartz)
ii. 55 mm sample discs (standard)
iii. 250-micrometer mesh sieve
iv. Distil water
v. Stiff brush
vi. 50 ml centrifuge tube
vii. Carbide or diamond glass scriber
viii. A spatula
ix. Hexane
x. Ethanol
xi. Sample cups and cylindrical agate grinding elements
xii. Weighing paper

Appendix 2. XRD and EDX machine settings

Bragg-Brentano system is recommended for optimum resolution at maximum intensity for XRD-machine.

Appendix Table 1. **Instrument parameters settings for XRD-machine**

Instrument parameter	**setting**
Geometry	θ/θ
Radiation Anode	Cu ($Cu_{k\alpha 1}$=0.154060 nm)
Generator	10 mA, 30 kV (commended)
Divergence slit	0.6 mm
Axial Soller slit module	Secondary 2.5 mm, primary 2.5 mm
Monochromatization kβ-filter	0.5 Ni filter
Linear LYNXENE detector	5 degrees detector opening and Ni-filter (0.5 %), Lower and upper discriminator window at 0.160^0 and 0.240^0
Achievable peak width	$<0.05^0$
Max. usable angular range	-3…..160^0 2θ
Instrument type	Portable desktop
Accuracy	± 0.02^0 for all measuring range
Alignment	Not required, factory aligned
Detector	Scintillation counters 1-dimensional LYNXEYE
Computer	Built-in optional PC connected via interface
Power supply	90-250 V
External cooling water supply	None
Exterior Dimension	70:61:60 (w:h:d)
Weight	95 kg
interfaces	2 x USB and LAN

***Appendix Table 2*. Instrument parameters settings for EDX-machine**

X-ray generator	
x-ray tube target	Rh
Tube voltage	5 to 50 kV
Tube current	1 to 1000µA
Cooling method	Air cooling (with fan)
Exposure area	10 mm dia. (standard) (automatic switching between 4 settings: 1, 3, 5, and 10 mm dia.)
Primary filter	Automatic switching between 5 types
Detector	
Type	Si (Li) semiconductor detector
LN_2	Only during measurement
LN_2 Dewar capacity	3L
LN_2 consumption	Approx. 1L/day

Appendix 3. Tables

Appendix Table 3. **Amount in percentage of minerals present in side-river sands**

Sample name	Albite	Diopside	Hornblende	Microcline	Quartz	Magnetite	Ilmenite
s10 (site 6)	19.2	0	21	0	37.3	10.9	11.6
s11 (site 7)	18.8	0	19.9	13.9	32.6	5.3	9.5
s12 (site 8)	14.1	4.9	19.4	0	58.3	0	3.2
s13 (site 9)	27.3	0	17.8	0	44.5	3.1	7.3
s14 (site 10)	22.6	4.2	19.1	0	49.3	0	4.8
Max	27.3	4.9	21	13.9	58.3	10.9	11.6
Min	14.1	0	17.8	0	32.6	0	3.2
mean	20.4	1.82	19.44	2.78	44.4	3.86	7.28
std. dev.	4.9	2.5	1.2	6.2	10.1	4.5	3.4

Appendix Table 4. **Amount in percentage of minerals present in mid-river sands**

Sample name	Albite	Diopside	Hornblende	Quartz	Orthoclase	Ilmenite
m4 (site 1)	22	6.8	10.2	61	0	0
m13 (site 2)	17.1	4.6	9.6	68.7	0	0
m22 (site 3)	27.9	4.1	13.9	51.6	0	2.5
m31 (site 4)	23.7	4.2	8.6	63.4	0	0
m40 (site 5)	19.1	6.2	9.3	60.2	5.3	0
Max	27.9	6.8	13.9	68.7	5.3	2.5
Min	17.1	4.1	8.6	51.6	0	0
mean	22.0	5.2	10.3	61.0	1.1	0.5
std. dev.	4.2	1.2	2.1	6.2	2.4	1.1

Appendix Table 5. **Specific activities of radionuclides present in the heavy sands in Bq Kg^{-1}. BDL=Below Detection Limit**

Site No.	Location	^{238}U		^{232}Th		^{40}K	
		Surface	Sub-surface	Surface	Sub-surface	Surface	Sub-surface
1	right	14.03	BDL	411	143	399	124
	center	8.28	9.41	314	484	195	348
	left	10.93	6.79	225	145	524	509
2	right	BDL	6.41	156	154	262	374
	center	BDL	BDL	143	143	168	181
	left	BDL	BDL	37.7	165	258	231
3	right	BDL	7.00	85.6	238	205	420
	center	BDL	11.2	6.12	289	186	461
	left	7.12	7.85	289	178	197	303
4	right	6.87	BDL	139	72.4	649	208
	center	7.34	6.15	177	144	191	501
	left	12.52	BDL	375	69.3	444	222
5	right	9.94	11.72	259	252	208	528
	center	5.40	9.66	82.5	175	233	535
	left	BDL	8.20	83.1	280	235	370
6	right	6.74	10.72	322	355	155	501
	center	11.46	6.30	389	138	459	517
	left	-	BDL	-	56.4	-	253
	max	14.03	11.7	411	484	649	535
	min	5.40	6.15	6.12	56.4	155	124
	mean	9.15	8.45	205	193	292	366
	std. dev.	2.78	2.03	128	108	146	137

***Appendix Table 6*. EDX analysis results of heavy metals in river sands in µg g^{-1}**

Site No.	Position	Iron (Fe)			Titanium (Ti)			Vanadium (V)		
		Surface	Sub-surface	Deep-surface	Surface	Sub-surface	Deep-surface	Surface	Sub-surface	Deep-surface
1	right	18708	52833		2283	8908		81.5	344	
	center	42208	58792	31500	9058	10908	4463	448	586	102
	left	25708	65375		3238	15458		205	733	
2	right	26917	34708		2788	5642		110	262	
	center	30083	29375	35625	6004	2479	5129	219	71.3	206
	left	39333	41208		9550	5304		329	330	
3	right	26625	18938		4238	1944		172	54.9	
	center	50292	40417	29792	12775	4379	2413	598	158	112
	left	29500	26792		4796	2971		264	142	
4	right	24188	16125		3269	1550		194	105	
	center	19500	27250	29167	2200	1821	2579	121	60.9	146
	left	23375	34250		3179	5742		110	246	
5	right	23375	73500		3081	14125		113	609	
	center	27188	76000	48458	3350	20438	9496	134	988	525
	left	42917	47083		8388	7358		435	317.5	
	max	50292	76000	48458	12775	20438	9496	598	988	525
	min	18708	16125	29167	2200	1550	2413	81.5	55	102
	mean	29994	42843	29090	5213	7268	4013	236	334	218
	std. dev.	9341	18965	15940	3229	5687	3232	153	278	176

Cont.…of Table 6

Site No.	Position	Manganese (Mn)			Chromium (Cr)			Copper (Cu)		
		Surface	Sub-surface	Deep-surface	Surface	Sub-surface	Deep-surface	Surface	Sub-surface	Deep-surface
1	right	455	1033		313	396		44.5	61.1	
	center	929	1149	1033	360	392	330	50.7	67.8	53.0
	left	653	1187		290	311		41.4	74.2	
2	right	729	810		258	310		45.5	55.6	
	center	630	929	766	223	223	203	38.5	61.9	39.8
	left	818	755		268	202		63.0	55.5	
3	right	570	409		215	252		42.8	44.1	
	center	978	1638	1529	268	189	179	57.7	82.0	43.0
	left	640	831		213	281		45.5	52.9	
4	right	444	466		230	181		36.0	41.8	
	center	425	956	750	236	202	228	38.7	42.1	40.5
	left	505	765		230	263		33.8	42.3	
5	right	708	1261		258	289		54.6	71.8	
	center	693	1284	892	224	181	288	38.2	58.4	53.1
	left	904	1092		303	314		52.7	52.0	
	max	978	1638	1529	360	396	330	63.0	82	53.1
	min	425	409	750	213	181	179	33.8	41.8	39.8
	mean	672	971	994	259	266	245	45.6	57.6	45.9
	std. dev.	177	320	320	42.2	70.9	62.5	8.52	12.5	6.66

Cont….. Of Table 6

Site No.	Position	Zinc (Zn)			Cobalt (Co)			Strontium (Sr)		
		Surface	Sub-surface	Deep-surface	Surface	Sub-surface	Deep-surface	Surface	Sub-surface	Deep-surface
1	right	30.4	86.7		107	418		325	265	
	center	56.1	68.8	44.4	277	545	219	341	273	298
	left	44.5	84.2		174	505		291	430	
2	right	43.5	57.9		166	193		315	329	
	center	42.8	50.5	46.8	160	204	235	397	332	354
	left	44.0	44.4		431	328		519	275	
3	right	45.8	39.0		168	151		346	399	
	center	79.9	52.1	34.0	355	298	190	487	473	363
	left	54.8	41.9		182	166		385	319	
4	right	43.0	23.3		141	102		351	352	
	center	32.4	39.4	42.2	106	165	190	365	310	351
	left	35.6	53.3		145	237		339	350	
5	right	45.0	95.5		135	553		417	320	
	center	38.3	82.5	65.0	167	537	320	370	322	309
	left	70.2	57.6		277	308		547	315	
	max	79.9	95.5	65.0	431	553	320	547	473	363
	min	30.4	23.3	34.0	106	102	190	291	265	298
	mean	47.1	58.5	46.5	199	314	231	386	337	335
	std. dev.	13.4	20.9	11.4	93.9	160	53.5	75.7	58	29

Cont….. of Table 6

Site No.	Position	Zircon (Zr)			Lead (Pb)		
		Surface	Sub-surface	Deep-surface	Surface	Sub-surface	Deep-surface
1	right	111	287		1.77	2.50	
	center	352	312	131	3.72	4.00	5.15
	left	133	703		4.53	3.27	
2	right	158	194		2.52	2.01	
	center	271	128	239	1.72	0.77	5.07
	left	452	250		4.57	5.90	
3	right	208	154		3.91	3.76	
	center	785	231	172	6.75	4.42	3.52
	left	188	187		4.58	1.28	
4	right	147	100		2.69	2.84	
	center	110	107	159	2.42	2.46	1.57
	left	145	240		4.46	1.98	
5	right	155	603		6.44	10.1	
	center	166	701	267	1.17	7.82	3.39
	left	463	242		4.82	3.51	
	max	785	703	267	6.75	10.1	5.15
	min	110	100	131	1.17	0.77	1.57
	mean	256	296	194	3.74	3.78	3.74
	std. dev.	187	204	57.0	1.67	2.51	1.47

***Appendix Table 7*. Mean concentrations of heavy metals in side-river sands in µg g^{-1} unless stated otherwise**

S. No.	Sample	Fe (%)	Ti (%)	V	Mn	Cr	Cu	Zn	Co	Sr	Zr	Pb
6	JS-de	3.6042	0.3963	66.0	1425	288	62.6	42.2	277	437	223	4.85
7	16-de	34.2083	7.4458	5371	4621	476	232	417	4329	348	4204	55.8
8	17-de	28.2500	7.7417	5500	4438	536	243	376	3213	398	2671	21.4
9	18-de	10.8917	3.5125	2121	2533	397	83.0	126	942	577	1483	16.4
	max-de	34.2083	7.7417	5500	4621	536	243	417	4329	577	4204	55.8
	min-de	3.6042	0.3963	66.0	1425	288	62.6	42.2	277	348	223	4.85
	$\bar{X}$-de	19.2385	4.7741	3264	3254	424	155	240	2190	440	2145	24.6
	Std. dev.-de	14.3690	3.4977	2644	1542	107	95.6	184	1901	98.5	1698	21.9

Appendix Table 8. **Enrichment factors (EF) and Geo-accumulation indices (Igeo) of heavy metals**

	Fe	**Ti**	**V**	**Mn**	**Cr**	**Cu**	**Zn**	**Co**	**Sr**	**Zr**	**Pb**
C_S(*µg g^{-1}*)	36203	6037	275	846	260	51	51	253	358	264	3.75
C_{NS}(*µg g^{-1}*)	36203	36203	36203	36203	36203	36203	36203	36203	36203	36203	36203
C_{SH}(*µg g^{-1}*)	47200	4600	130	850	90	45	95	19	170	160	20
C_{NSH}(*µg g^{-1}*)	47200	47200	47200	47200	47200	47200	47200	47200	47200	47200	47200
C_S*	192385	47741	3264	3254	424	155	240	2190	440	2145	24.6
C_{NS}*	192385	192385	192385	192385	192385	192385	192385	192385	192385	192385	192385
EF	1	1.71	2.76	1.30	3.77	1.48	0.70	17.4	2.75	2.15	0.24
I_{geo}	-0.97	-0.19	0.50	-0.59	0.95	-0.40	-1.48	3.15	0.49	0.14	-3.00
EF*	1	2.55	6.16	0.94	1.16	0.85	0.62	28.3	0.63	3.29	0.30
I_{geo}*	1.44	2.79	4.07	1.35	1.65	1.20	0.75	6.26	0.79	3.16	-0.29

where C_S is the sample's metal concentration, C_{NS} is the sample's normalizing metal (Fe) concentration, C_{SH} is the average shale's metal concentration and C_{NSH} is the average shale's normalizing metal (Fe) concentration. Parameters with an asterisk represent the side-river sand samples. All the metal concentrations are in µg g^{-1}.

Appendix Table 9. **Selected heavy metals from Wisconsin Guidelines on Consensus-Based Sediment Quality of 2003**

Heavy Metal	Concentration in mg kg^{-1}
Iron	20000
Manganese	460
Zinc	120
Chromium	43
Lead	36
Copper	32
Nickel	23
Arsenic	9.8